

1 **Effects of Storm Surge Barrier Closures on Estuary Saltwater Intrusion and**
2 **Stratification**

4 **Ziyu Chen^{1*}, Philip M. Orton^{1*}**

5 ¹Department of Civil, Environmental and Ocean Engineering, Stevens Institute of Technology,
6 Hoboken, NJ, 07030, USA

7 Corresponding author: Philip M. Orton (porton@stevens.edu), Ziyu Chen
8 (zchen44@stevens.edu)

9 **Key Points:**

- 10 • Multi-day gate closures can increase saltwater intrusion and stratification past historical
11 maxima
- 12 • Recovery time to normal conditions after re-opening depends on closure duration,
13 streamflow and estuary length
- 14 • Closure frequency should be limited in order to prevent durable estuary physical changes
15 from inadequate recovery time

This is the author manuscript accepted for publication and has undergone full peer review but has not been through the copyediting, typesetting, pagination and proofreading process, which may lead to differences between this version and the [Version of Record](#). Please cite this article as doi: [10.1029/2022WR032317](https://doi.org/10.1029/2022WR032317).

This article is protected by copyright. All rights reserved.

16 Abstract

17 Gated storm surge barriers have been constructed or proposed in many estuaries worldwide for
18 coastal flood risk reduction. Past studies have shown that, even when open, a barrier system's
19 fixed infrastructure can increase estuary stratification and salt intrusion, potentially affecting
20 water quality and ecological processes. However, surge barrier closures could have a much
21 stronger influence on estuary conditions by temporarily blocking the tidal exchange. In this
22 project, we use an existing regional three-dimensional hydrodynamic model, with modifications
23 to simulate surge barrier closure and re-opening, to study the effects on estuarine salt intrusion
24 and stratification of the Hudson River. Across a range of modeled scenarios of gate closure
25 frequencies, durations and river streamflows, we evaluate the changes caused by gate closures, as
26 well as the recovery time to normal conditions. Our results for the Hudson show long-duration
27 gate closures (three or more days) with low streamflows temporarily lead to salt intrusion and
28 stratification beyond recent historical extremes. Moreover, monthly frequency closures, which
29 could occur as soon as 2070 under realistic scenarios of sea-level rise and barrier management,
30 do not allow for recovery under low streamflow conditions and could lead to durable changes to
31 estuary physical conditions. As a result, long duration closures and high frequency closures both
32 constitute a threat to municipal water supplies. This study demonstrates a framework for
33 understanding the potential impacts of any proposed surge barrier system and can help improve
34 our understanding of corresponding ecological impacts.

35
36 **Keywords:** storm surge barrier; saltwater intrusion; stratification; estuary; freshwater resources; Hudson River

37

38 1 Introduction

39 Storm surge is one of the most catastrophic events among all natural disasters. It can cause a
40 large number of fatalities as well as enormous economic losses in a single event. Moreover,
41 coastal flood events are predicted to be more frequent and intense under sea-level rise (SLR) and
42 climate driven changes in storm characteristics (Lin et al., 2012; Marsooli et al., 2019). Repeated
43 record-setting years for hurricane damages are accelerating interest to investigate diverse
44 engineering approaches for coastal flood risk reduction, including shoreline-based measures,
45 natural and nature-based features and closable storm surge barriers or tide gates. Storm surge
46 barriers or tide gates can effectively protect harbors and minimize flooding, property damage,
47 and loss of life during large storms. They can be one of the most cost-effective approaches to
48 mitigate the effects of flood hazards (Deltacommissie, 2009; National Research Council, 2014).
49 An increasing number of storm surge barriers has been constructed and applied for flood
50 protection worldwide (Mooyaart & Jonkman, 2017). Recently, storm surge barriers have been
51 proposed for construction on many U.S. estuaries, including New York (NY)/New Jersey (NJ)
52 Harbor (USACE, 2019), Boston Harbor (Kirshen et al., 2018), Galveston Bay/Houston (USACE,
53 2020b), coastal New Jersey (USACE, 2021a), Miami (USACE, 2020c) and Norfolk (USACE,
54 2017).

55 Surge barriers typically span the opening to a harbor or river mouth with gates in the barriers left
56 open under normal conditions to allow exchange of water due to the tides. Past studies have
57 shown that when the surge barriers are left open, due to their fixed infrastructure obstructing a
58 portion of the estuary cross-section, they can reduce tidal exchange and cause increases to

59 stratification and salt intrusion length (e.g., Du et al., 2017; Orton & Ralston, 2018; Ralston,
60 2022). These physical changes can affect water quality, ecological processes, sediment transport
61 and other environmental aspects of an estuary (e.g., Bakker et al., 1990; Swanson et al., 2013).
62 Gate closures may have a stronger impact on estuary conditions by completely stopping the tidal
63 currents during the period of closure. Moreover, SLR can cause increased frequency of surge
64 barrier closures and closure duration to prevent flooding, which will intensify the gate closure
65 impacts (Chen et al., 2020). Already this has occurred with some constructed surge barriers (e.g.,
66 Thames Barrier in Britain, Lavery & Donovan, 2005; New Bedford Barrier in Massachusetts,
67 Orton et al., 2022; Stamford barrier in Connecticut, USACE, 2021b). However, there have been
68 no prior academic studies focused on modeling surge barrier closure effects.

69 Municipal water supplies in tidal rivers are increasingly threatened by salt intrusion due to
70 climate change and dredging, which both can shift the salt front landward (e.g., Leuven et al.,
71 2019; Yuan & Zhu, 2015). The historical records of abnormal estuarine salt intrusion and
72 contamination of drinking water supplies typically show correlation with severe drought events
73 (e.g., Bowen & Geyer, 2003). For some estuaries, increased salt intrusion also results from
74 declining runoff due to climate change (e.g., Akter et al., 2019; Cloern et al., 2011). These
75 effects could gradually increase the risk of salt contamination of upstream municipal water
76 intakes. Surge barrier systems could further threaten upriver freshwater resources from both their
77 open barrier effects and the gate closure operations for flood protection.

78 Similarly, evidence shows that climate change is worsening hypoxia in some estuaries due to
79 rising sea levels, warming water temperatures and changes in streamflow, precipitation and/or
80 wind patterns (e.g., Cottingham et al., 2018; Du et al., 2018; Ni et al., 2019). Surge barrier
81 systems could worsen this trend by increasing the stratification and reducing and temporarily
82 terminating the estuary vertical mixing. There is uncertainty how these combined effects could
83 affect the estuary water quality.

84 Storm surge barriers are being evaluated by the US Army Corps of Engineers in its Harbor and
85 Tributaries (HAT) Study for coastal storm risk management for the NY metropolitan area
86 (USACE, 2019). The USACE estimates that coastal flood risk is very high in the region, at \$5.1
87 billion average annual damages per year in 2030, leading to high benefit-cost ratios ranging from
88 2.1-4.6 for various surge barrier plans (USACE, 2020a). Two specific risk reduction alternatives
89 being studied (Alternatives 2 and 3A) include surge barrier systems that would affect the
90 Hudson River estuary and its many sub-estuaries. We recently held a series of stakeholder
91 workshops that identified several specific concerns around prospective surge barriers, including
92 excessive salt intrusion that could affect freshwater intakes that are normally only affected
93 during drought conditions, and the potential for increased stratification of the eutrophic waters
94 contributing to hypoxia in the Hudson or its adjoining estuaries (e.g., Orton et al., 2020).

95 In this paper, we study the effect of closed surge barriers on estuary physical conditions and use
96 the hypothetical NY/NJ Harbor barriers and Hudson River estuary as a case study. The goals of
97 this research are:

- 98 1. Quantifying the influences of storm surge barrier closures on estuary saltwater intrusion and
99 stratification
- 100 2. Assessing the recovery time after the gates reopen, with application to understanding the
101 maximum closure frequency

102 3. Identifying any extreme physical conditions induced by episodic operations of surge barriers
103 that could cause new unexpected environmental issues

104 4. Recommending model experiments and metrics for evaluating other constructed/proposed
105 barriers

106 Below, Section 2 introduces the study site and methods of the surge barriers closure modeling,
107 Section 3 shows the results of closed surge barrier effects on the Hudson River estuary, and
108 Section 4 discusses the generality of the surge barriers closure analysis with respect to different
109 types of estuaries and the barrier management implications from this research. In Section 5 we
110 summarize the primary conclusions of this research.

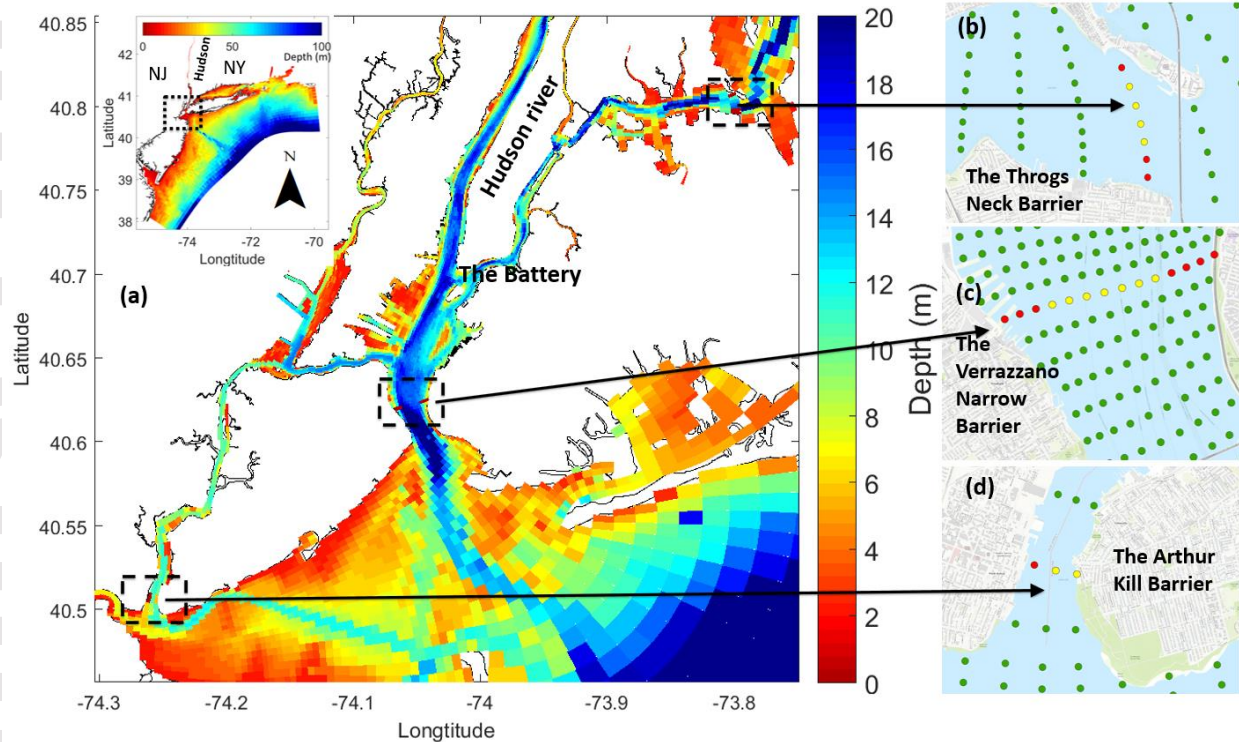
111 **2 Study site and Methods**

112 2.1 Hudson River Estuary and NY/NJ Harbor

113 The Hudson River Estuary and several other sub-estuaries and tide straits branch out from
114 NY/NJ Harbor (Panel a in Figure 1). The Hudson, a 245 km long estuary and tidal river, is one of
115 the most well-studied estuaries in the world regarding salt intrusion, salt stratification, estuary
116 adjustment time, sediment transport and a wide range of other topics (Levinton et al., 2006). It is
117 a relatively simple channelized estuary with limited wind effects and typical variations in salinity
118 and stratification being predominantly controlled by river streamflow and fortnightly (spring-
119 neap) and monthly (perigee-apogee) modulations in tidal forcing (e.g., Ralston et al., 2008).
120 Resulting character varies between partially-mixed, strongly stratified and salt-wedge estuary
121 types (e.g., Geyer & MacCready, 2014). Observations at the Battery tide gauge (southern
122 Manhattan, New York City) show the tide is principally semi-diurnal and the mean tidal range is
123 1.4 m (Ralston & Geyer, 2017), varying from about 1 to 2 m (Orton & Visbeck, 2009). The
124 Hudson is tidal from Manhattan to the Green Island dam at Troy, NY, and receives fresh water
125 mainly from north of Troy (e.g., the Mohawk River) plus multiple smaller tributaries along the
126 Hudson (Orton et al., 2012). Future climate change is expected to alter streamflow conditions by
127 increasing the mean streamflow but also reducing the streamflow during the dry season (Schulte
128 et al., 2017). Also, estuary temperatures will be warmed by regionally warming atmospheric
129 temperatures.

130 Communities surrounding NY/NJ Harbor are vulnerable to coastal flooding due to storm surge
131 and high tides and sometimes compound coastal-pluvial flooding (e.g., Hurricane Irene; Wahl et
132 al., 2015). This estuary area also suffers from a high relative SLR rate due to subsidence (Kopp et
133 al., 2014), which causes more severe and frequent flood hazards (e.g., Orton et al., 2019).

134



135

136 **Figure 1.** (Panel a) The NY-NJ Harbor-Estuary is shown with the proposed locations of the
 137 Alternative 3A storm surge barriers (Verrazano barrier, Arthur Kill barrier, Throgs Neck
 138 barrier); (Panel a top left) The NYHOPS model domain stretches from Maryland to Cape Cod
 139 and is centered on the NJ and NY coastal zone and estuaries. Color shading represents model
 140 bathymetry with modified model grids for fixed barriers in Panel a. Panel b-d are the maps for
 141 the 3 proposed storm surge barriers; Green dots show grid cell centers, red dots represent fixed
 142 surge barrier components and yellow dots represent gates (or the aggregate area of several open
 143 gates).

144 2.2 Three-dimensional hydrodynamic model with closable gates

145 Computational modeling of estuary physical conditions is performed using the three-dimensional
 146 Stevens Estuarine and Coastal Ocean Model (sECOM) (Georgas & Blumberg, 2010). The model
 147 is applied on the New York Harbor Observing and Prediction System (NYHOPS) domain/grid
 148 including the Mid-Atlantic and Northeastern U.S. coastline from Maryland to Rhode Island .
 149 This model and domain have been applied in a forecast system since 2007 to provide accurate
 150 real-time water property forecasts (<http://stevens.edu/NYHOPS>) and probabilistic coastal-fluvial
 151 flood forecasts (Jordi et al., 2019). Streamflow is incorporated into the model including all
 152 tributaries of the region's waterways. For those tributaries without observations, freshwater
 153 inputs are also taken into account by scaling from nearby streamflow gauge data and the relative
 154 watershed area ratios (Georgas & Blumberg, 2010; Orton et al., 2012). The sECOM-NYHOPS
 155 model is well-validated in forecast (Georgas & Blumberg, 2010) and hindcast modes with
 156 typical hindcast RMSEs of 0.10 m, 1.2 °C and 2.3 psu for total water levels, temperature and
 157 salinity, respectively (Georgas, Yin, et al., 2016). Also, the model provides accurate estimates of
 158 the Hudson River salt front location ($r^2 = 0.83$; Georgas & Blumberg, 2011).

159 One of the storm surge barrier system scenarios being studied in the HAT Study (Figure 1)
160 (Alternative 3A; USACE, 2019) is represented in the model as a combination of fixed immobile
161 (“fixed”) flow-obstructing barriers and closable gates. Grid cells are chosen to represent these
162 features, with bathymetry data at blockages being altered to raise it high above sea level,
163 blocking water flow. We revised the model code to enable scheduled gate closures and openings
164 during a model simulation. The representations of the barriers and their gates are simplified,
165 given our model’s ~140 m across-channel resolution only typically has about 10-15 cells across
166 the Verrazzano Narrows and Hudson River estuary channels. As a result, we only model open
167 gates as wide-open spaces, and we do not resolve separate navigation gates (2) and auxiliary
168 flow gates (several) that exist in the USACE designs, the latter of which at 46 m width (Ralston,
169 2022) would require resolutions of about 5-10 m to accurately capture. The potential approaches
170 for closing and opening these different types of gates is later discussed in Section 4. Two prior
171 studies have modeled open surge barrier effects on the Hudson. One preliminary study of surge
172 barriers evaluated effects of a barrier at a different location further offshore but with similar
173 coarse representations (Orton & Ralston, 2018). The other modeled the potential Verrazzano
174 barrier using a nested grid with refined resolution of 20 m (Ralston, 2022).

175 For the Verrazzano barrier (Figure 1, Inset C), we capture the aggregate open cross-sectional
176 area reasonably with 7 neighboring cells. This is the dominant water pathway for flow into
177 Upper New York Bay and the Hudson. The modified surge barrier model digital elevation
178 model (DEM) with fixed barriers and open gates is shown Figure 1. This model DEM has an
179 approximate 58.7% gated flow area (GFA; cross-sectional area open to flow, as a percentage of
180 that of the unobstructed natural system) at the Verrazzano barrier, to approximately match the
181 USACE design’s value of 59% at that location (USACE, 2019).

182 We more coarsely represent the two other barriers and their gates (Figure 1, Insets B and D
183 respectively), although these have a much smaller effect on the Hudson, the focus of our study.
184 Our barriers have a 4-cell wide 57.4% GFA at Throgs Neck (USACE: 62%) and a 2-cell wide
185 62.7% GFA at Arthur Kill (USACE: 47%). These two locations have smaller cross-sectional
186 areas than the Verrazzano (Throgs Neck <50%, Arthur Kill <15%), and their flows do not enter
187 directly into the Hudson.

188 We did not mimic the “concrete sill design” (a normal component of a surge barrier system
189 under the gates; e.g., Mooyaart & Jonkman, 2017; USACE, 2019) in our model DEM at the open
190 gate locations because the model’s relatively coarse grid resolution of the gated flow areas
191 already has smooth bathymetry that is similar to the concrete sill.

192 2.3 Model experiments and forcings

193 We simulate estuary physical conditions under 21 different scenarios summarized in Table 1 and
194 described in detail below. To create the most realistic simulations, model initial conditions and
195 boundary conditions are taken from the NYHOPS operational forecasts, typically from the
196 hindcast period (24 hours at the start of each forecast period). This includes realistic tidal forcing
197 with 9 constituents (K1, O1, Q1, M2, S2, N2, K2, M4, M6) to capture both the spring-neap and
198 perigee-apogee variabilities. The experiments include cases that utilize idealized constant
199 forcings or realistic historic events. These detailed spatiotemporal data are briefly summarized
200 below and made available in the Supplementary Materials (SM). Additional experiments to

201 quantify sensitivity to factors such as SLR and dredging are also summarized below (Section
202 2.5) and presented in detail in the SM.

203 When the barriers are open, the fixed barrier components can reduce the tidal amplitude of the
204 estuary, which will in turn increase salt stratification and intrusion length (Orton & Ralston,
205 2018; Ralston, 2022). So, we run both “Without-Barrier” (NYHOPS DEM) and “Open-Barrier”
206 (with fixed barriers DEM) scenarios to investigate the physical impact of the fixed barriers, and
207 the latter is the “Control” simulation for comparison with gate closure conditions. Also, to study
208 the gate closure effects, we use a range of tide- and storm-driven flood simulations with various
209 gate closure frequencies, gate closure durations and streamflow conditions.

210 We model 1, 3 and 5-day long gate closures because this represents the range of durations for
211 likely present and future high-tide flooding and storm surge events based on data from prior
212 studies (e.g., Orton et al., 2016; Orton et al., 2019). In cases where there are successive flood
213 threshold exceedances at high tides, even if the water level exceeds a flood datum briefly and
214 then drops below it, the large navigation gates for cross-harbor barriers cannot be opened and
215 closed within less than one tidal cycle (B. Wisemiller, USACE, pers. comm., 2021). An example
216 of a multi-day surge event is the 1992 Nor’easter and if a similar event were to occur with 50 cm
217 of SLR it would have 8 tide cycles exceeding moderate flood datum at Manhattan (Chen et al.,
218 2020). A prior USACE-directed study of surge barriers for a nearby area similarly included a 4-
219 day closure scenario for surge barrier closure experiments (NYC-DEP, 2016). We discuss
220 management approaches proposed by the USACE to reduce these durations in Section 4.

221 Two types of flood scenarios are characterized in the model experiments. “Coastal-Flood”
222 scenarios are simulated with tides only and no storm surge, representing both spring tide
223 flooding events and storm surge flooding events with low or moderate rainfall. Both scenarios
224 are captured in the same set of simulations because (a) local winds have only a minor effect on
225 the Hudson, which is narrow and relatively sheltered from wind, and (b) any storm surge would
226 be blocked by the surge barriers and have no effect on the Hudson conditions. Moreover, typical
227 storm surges only have a minor effect on Hudson salinity and salt intrusion, as tides comprise an
228 equal or larger component of total water level variability. Tidal flooding is presently only a
229 factor at perigean (“King”) tides in a few neighborhoods of the harbor-estuary region (Orton et
230 al., 2015), but will become more frequent and widespread with SLR (Orton et al., 2019). In these
231 simulations, we consider the spring-neap-king tide variations at the open boundary conditions to
232 capture realistic conditions in a broad sense.

233 A “Compound-Flood” scenario with storm surge, high streamflow and heavy rain-on-water was
234 also studied, using the realistic scenario of tropical storm Irene (2011). While our recent research
235 showed that such compound events have a very low probability of causing trapped water
236 flooding (Chen et al., 2020), here we quantify and study the role of simultaneous rain on the
237 surge barrier closure effects on the estuary saltwater intrusion and stratification. Irene modeling
238 methods are explained in detail in Orton et al. (2012).

239 Streamflows for the Coastal-Flood scenarios are characterized by using a temporally-constant
240 “Mean-Streamflow” case to represent average conditions, and a “Low-Streamflow” case to
241 represent typical dry season conditions. The Mean-Streamflow case of 404 m³/s (Table 1) is
242 approximately equal to the USGS observed daily average streamflow at Green Island gauge

243 (USGS 01358000) from 1947 to 2019 ($409 \text{ m}^3/\text{s}$). The Low-Streamflow case at the Green Island
 244 ($150 \text{ m}^3/\text{s}$) is also close to the median of observed daily average streamflow during dry season
 245 (July to September) from 1947 to 2019 ($156 \text{ m}^3/\text{s}$). Other Hudson tributaries are similarly
 246 characterized by mean and low streamflow estimates in the simulations. For comparison, the
 247 time-varying streamflow during Irene was $2800 \text{ m}^3/\text{s}$ over a three-day period and $1200 \text{ m}^3/\text{s}$ over
 248 a 30-day period (Figure S1). For further discussion of historical streamflow data supporting these
 249 choices, see Section SM Text S3.

250 The idealized Coastal-Flood scenario gate closures are centered on the peak of spring tide. For
 251 the NY/NJ Harbor-Estuary region, extratropical cyclones cause small-to-moderate but often
 252 long-duration storm surges that are relatively reliant on high tides to cause flooding. As a result,
 253 coastal flooding during extratropical cyclones predominantly occurs at spring tides and can occur
 254 for several consecutive tidal cycles (Orton et al., 2015). This pattern could be worsened by SLR,
 255 for example with a long-duration storm surge (e.g., December 1992 nor'easter, Chen et al.,
 256 2020). The effects on our results of this spring tide assumption are evaluated in SM Text S2.2.

257 To mimic the realistic gate closure operation for 1/3/5-day flood events, we close the
 258 Verrazzano, Arthur Kill and Throgs Neck gates at slack tide before flood tide and reopen close
 259 to slack tide before ebb tide. We use initial simulations where the barrier is closed but not re-
 260 opened to learn the water rise rate for Low- and Mean Streamflow cases, then use that
 261 information to tune the timing of reopening to occur close to slack but when water levels are
 262 almost identical inside and outside the barriers. For the “Compound-Flood” scenarios, water
 263 inside the barrier system rises more significantly and there is a water level gradient present at the
 264 moment of opening the gates, as discussed below in Section 3.3.2.

265 Annual closure frequency is represented with the single-closure simulations, whereas a period of
 266 monthly closures is represented with the three-closure simulations (e.g., gates closed at spring
 267 tide in three consecutive months). For the sake of computational efficiency, we only run
 268 simulations for 150 days, which we find is enough to investigate the recovery of estuary physical
 269 conditions after closures for this system.

270 **Table 1.** Flood simulation scenarios with different closure duration, closure frequency,
 271 streamflow

<i>Flood Event</i>	<i>Streamflow (m^3/s)</i>	<i>Surge barriers operation</i>	<i>Closure Duration</i>	<i>Closure Frequency</i>
<i>Coastal Flood</i>	404	Without-Barrier	None	None
<i>Coastal Flood</i>	404	Open-Barrier (Control)	None	None
<i>Coastal Flood</i>	404	Gate-Closure	1/3/5 Days	Annual
<i>Coastal Flood</i>	404	Gate-Closure	1/3/5 Days	Monthly
<i>Coastal Flood</i>	150	Without-Barrier	None	None
<i>Coastal Flood</i>	150	Open-Barrier (Control)	None	None

<i>Coastal Flood</i>	150	Gate-Closure	1/3/5 Days	Annual
<i>Coastal Flood</i>	150	Gate-Closure	1/3/5 Days	Monthly
<i>Compound Flood (Irene)</i>	2800 ^a	Without-Barrier	None	None
<i>Compound Flood (Irene)</i>	2800 ^a	Open-Barrier (Control)	None	None
<i>Compound Flood (Irene)</i>	2800 ^a	Gate-Closure	1/3/5 Days	Annual

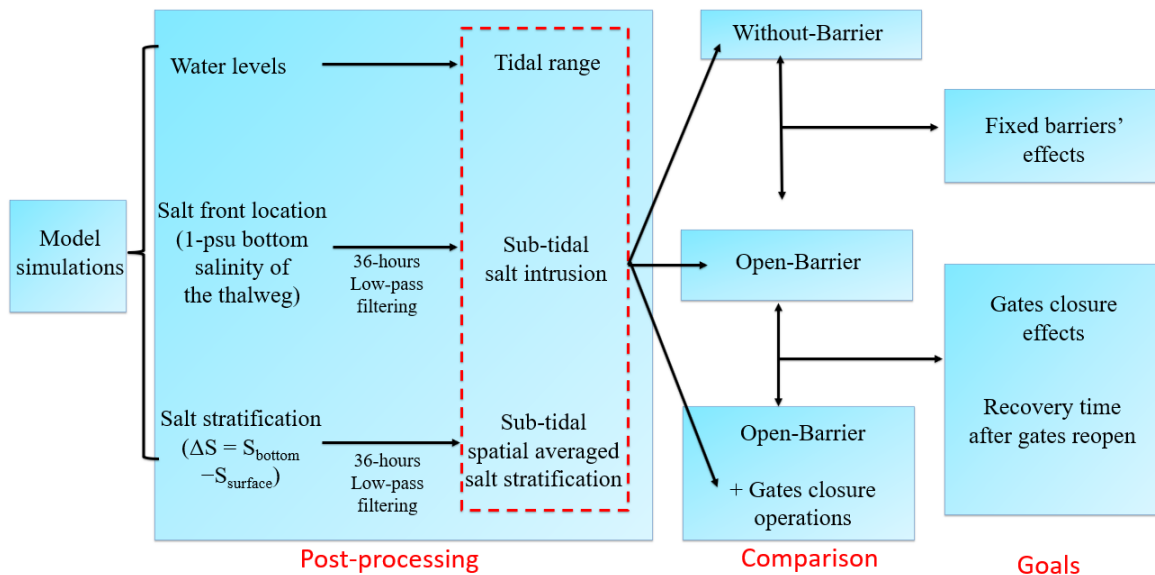
272 ^a The compound flood event scenario Irene utilized realistic time-varying streamflows, for
 273 which the 3-day average was 2800 m³/s

274 All simulations use appropriate initial conditions for periods with similar streamflows and
 275 salinity from our operational forecast system (Georgas, Blumberg, et al., 2016). For the
 276 Hurricane Irene (Compound Flood) simulation, we use initial conditions created from the
 277 operational simulation of that event, which requires only 2 days of spin-up time (Orton et al.,
 278 2012). For the idealized Coastal-Flood scenarios, we use the initial conditions from operational
 279 system simulations with similar conditions (for Mean- and Low- Streamflow scenarios) and
 280 include a 20-day spin-up time.

281 2.4 Post processing of salt intrusion and stratification

282 A summary diagram of the scientific methods for open and closed surge barrier effects on
 283 estuary conditions is shown below in Figure 2.

284



285

286 **Figure 2.** Diagram of the scientific analysis approach

287 The salt front is identified as the location of the 1-psu bottom isohaline in the Hudson's thalweg.
288 We used a 36-hour low-pass running-average filter on the modeled salt intrusion length to
289 remove the tidal signals and obtain the sub-tidal salt intrusion variation along the thalweg.
290 Recovery time is defined as the period of time required after gate reopening for the sub-tidal salt
291 intrusion length from a "Gate-Closure" scenario to be less than 3% to that in the Control
292 scenario.

293 We quantify stratification and its changes in three ways: (1) the spatial average salinity
294 difference between the bottom and surface layers ($\Delta S = S_{\text{bottom}} - S_{\text{surface}}$), (2) the spatial average
295 salinity vertical gradient [$(S_{\text{bottom}} - S_{\text{surface}})/\text{depth}$] computed on all saltwater grid cells behind the
296 barriers, and (3) the stratification at mid-estuary, defined as the thalweg location having a
297 vertically average salinity of 15 psu. However, hereafter we only refer to approach #1 in our
298 assessment of stratification changes because the other two approaches give similar results in this
299 estuary. This is because for estuaries with relatively constant water depths like the Hudson,
300 estuary-mean ΔS and $\Delta S/\text{depth}$ have very similar fractional variations. We define an "excess
301 stratification recovery time" for the estuary stratification as the period of time required after gate
302 reopening for the excess stratification in the Gate-Closure scenario to disappear compared with
303 the stratification in the Control scenario. After the gates are reopened, this is defined as being the
304 first time when the difference of sub-tidal spatial average stratification between the Gate-Closure
305 scenario and Control scenario is less than 0.

306 We compute the maximum stratification conditions along the thalweg from single gate closure
307 scenarios. Also, we compare these with the maximum stratification variation range during 1979-
308 2013 from a hindcast based on the NYHOPS model (Georgas, Yin, et al., 2016). The salt
309 stratification and intrusion increments (positive anomalies relative to the state before closing the
310 gates) by various durations of gate closures are also evaluated, which can be compared with
311 natural variability.

312 2.5 Sensitivity analyses

313 Several sensitivity tests were conducted, quantifying the effects of SLR, dredging, wind,
314 horizontal diffusion parameterization settings, and neap-spring phasing of closures on our
315 results. These methods and results are presented in detail in SM sections (Text S1-S2), and
316 briefly discussed in Section 4.

317 3 Results

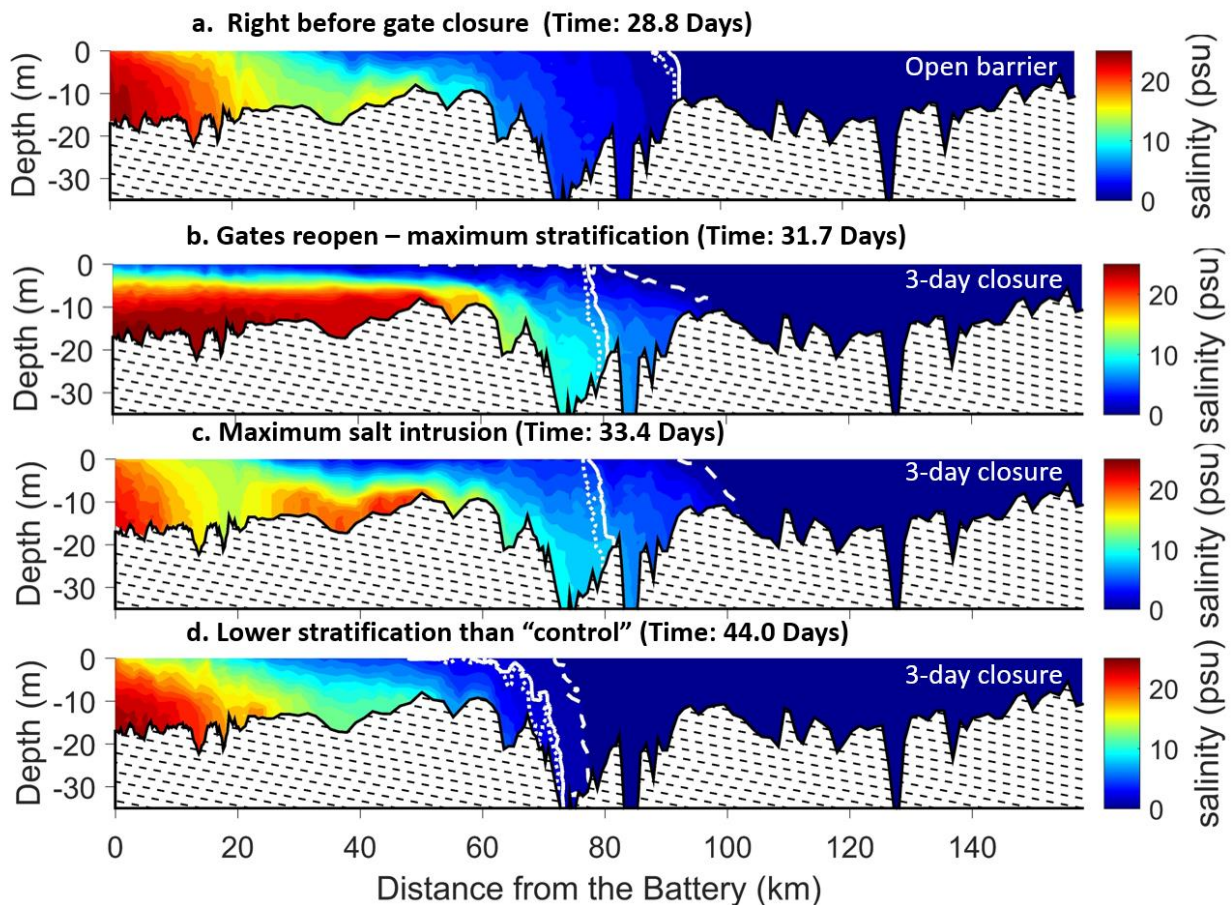
318 An example case of the influence of a surge barrier's open infrastructure, as well as the chain of
319 events surrounding a closure, are shown in Figure 3. Spatiotemporal salinity shade plots showing
320 full-duration simulation results for Control scenarios and all experiments given in Table 1 are
321 presented in order (from panel a to u) in Figure S2. Below, we present the baseline change
322 between Without-Barrier and Open-Barrier simulations (Section 3.1). We then contrast
323 spatiotemporal shade-plots of results for Open-Barrier sample versus Closed-Barrier results from
324 single 3-day gate closures and their recovery process (Section 3.2). We present detailed analyses
325 of single (annual) closure effects on saltwater intrusion and stratification and its recovery time
326 (Section 3.3). The monthly closure scenarios indicate more severe estuary effects, as there is
327 likely inadequate recovery time between the high frequent closures. These results are discussed

328 below but are only displayed in Figure S2 because they do not add to the demonstration already
 329 shown with single-closure cases below.

330 3.1 Fixed (open) storm surge barrier impacts

331 The model simulations indicate the Open-Barrier system (Alternative 3A) causes 0.1% to 4%
 332 (median is 3.2%) salt intrusion length extension and -1.4% to 7% (median is 1.3%) changes
 333 of salinity stratification compared with Without-Barrier system with constant Mean-Streamflow
 334 during a spring neap cycle. Also, there is about 3.0% average tide range reduction at the Battery
 335 in one lunar cycle, a similar reduction to that found in the modeling results from the HAT Study
 336 (USACE, 2020a). These results serve as our primary baseline or Control scenario, against which
 337 closures are compared.

338



339

340 **Figure 3.** Salinity profiles along the Hudson River thalweg during mean streamflow conditions
 341 from (a) the Alternative 3A Open-Barrier simulation and (b,c,d) 3-day Gate-Closure simulation
 342 at different simulation times. White lines in each figure are the 1 psu isohalines from
 343 simultaneous Without-Barrier simulation (dotted), Open-Barrier simulation (dashed) and Gate-
 344 Closure simulation (solid).

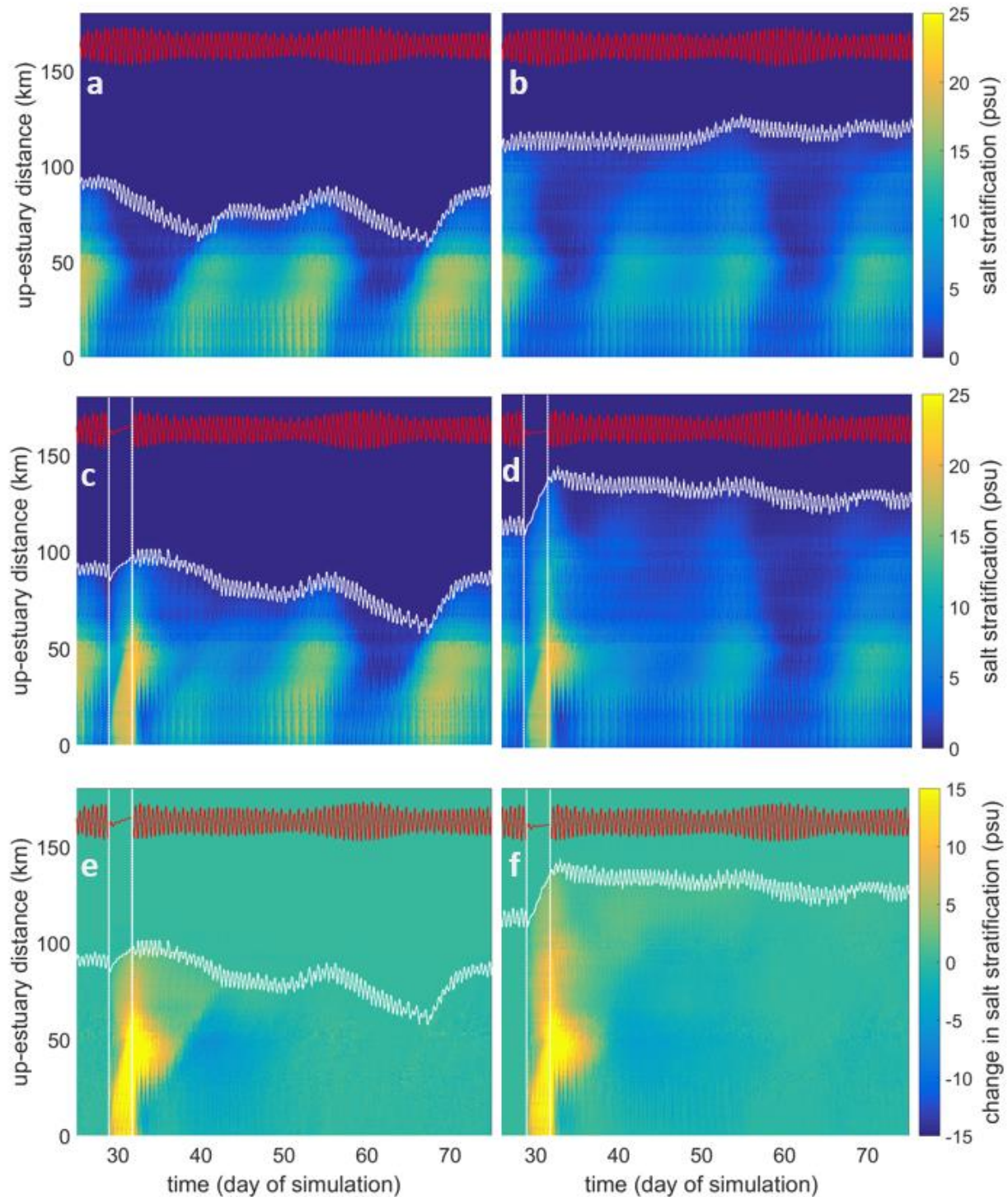
345 3.2 Spatiotemporal view of closed barrier impacts

346 3.2.1 Coastal flood events

347 Gate closures intended to prevent flooding have an intensified but temporary impact on estuary
348 conditions (e.g., Figure 3 for Mean-Streamflow conditions). The barrier closure stops the tidal
349 currents and associated vertical water column mixing throughout the estuarine areas behind the
350 barrier. The salt intrusion responds to its along-estuary density-gradient (baroclinic) forcing and
351 this lack of vertical mixing by propagating rapidly up-estuary (Figure 3b). A salt wedge slides
352 below fresher surface water with relatively little mixing, enhancing stratification relative to the
353 Open-Barrier case (compare horizontal and vertical 1 psu contour lines). After the gates are
354 reopened, tidal currents are re-instated but there remain high levels of stratification, so the salt
355 intrusion continues moving upstream for a brief period until it reaches its maximum (Figure 3c).
356 After continued vertical mixing and seaward advection, the salinity stratification and intrusion
357 gradually return toward their normal values (Figure 3d).

358 Figure 4 left-side panels (a,c,e) give a continuous spatiotemporal perspective on the modeled
359 salinity stratification and gate closure effects for Mean-Streamflow conditions. The Open-Barrier
360 (Control) scenario (panel a) shows the common pattern of periodic variations of salt intrusion
361 length and stratification with modulation of tides by the spring-neap cycle and lunar orbital
362 (perigee-apogee) phasing (e.g., Orton & Visbeck, 2009; Ralston et al., 2008). The barrier gate
363 closure (panel c, day 28.9) leads to increased stratification and migration of the salt front up-
364 estuary, and the re-opening of the gates (day 31.7) enables a gradual recovery. Shade plots of the
365 difference between Control and the Gate-Closure experiment show positive (yellow) and
366 negative (blue) anomalies and a recovery back to normal conditions (green for zero difference)
367 within about three weeks.

368



369

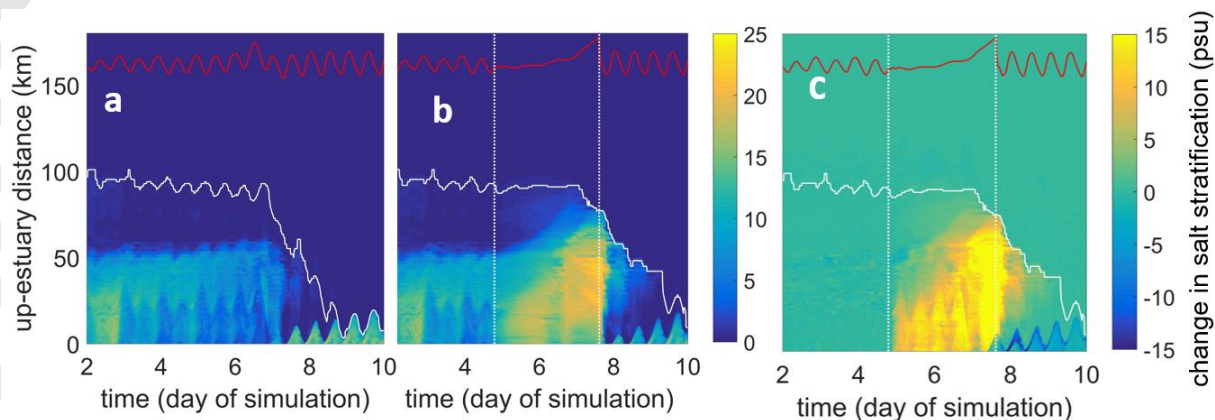
370 **Figure 4.** Spatio-temporal stratification and stratification change for the Hudson, with distance
 371 up-estuary from the Battery. The left column panels (a,c,e) show results for the Mean-
 372 Streamflow simulations, right column panels (b,d,f) show results for Low-Streamflow
 373 simulations. Color shading in the top row panels (a,b) shows modeled salinity stratification (ΔS
 374 $= S_{\text{bottom}} - S_{\text{surface}}$) for the Open-Barrier (Control) scenario and middle row panels (c,d) show

375 results for the single (annual) 3-day Gate-Closure scenario. Bottom row color shading represents
 376 the corresponding changes in salinity stratification (Gate-Closure scenario minus Open-Barrier
 377 scenario). White lines show the salt intrusion length, and red lines show the water level at the
 378 Battery with an arbitrary scaling. The vertical dashed lines show the time of gate closure or
 379 reopening.

380 The gate closure impacts have potential to overlap with the negative effects from possible low
 381 streamflow conditions during a dry-weather coastal flood event, which would lead to more
 382 extreme salt intrusion and stratification conditions. Contrasting mean (panels a,c of Figure 4) and
 383 low river discharge conditions (panels b,d), lower streamflow leads to a greater salt intrusion
 384 distance, a typical pattern for a river-estuary. When gate closure occurs under low streamflow
 385 conditions, it results in relatively slow recovery of the stratification and salt intrusion length
 386 (panel f). Historically, drought conditions with low streamflow can enable the salt intrusion to
 387 reach 120 km from the Battery, contaminating municipal freshwater intakes at Poughkeepsie
 388 (Bowen & Geyer, 2003). Gate closure could aggravate this salt intrusion problem – Figure 4
 389 shows an example that salt intrusion length could extend to about 140 km from the Battery.

390 3.2.2 Compound flood events

391 Gate closures during periods of high streamflow further illustrate a clear trend toward lesser
 392 salinity impacts and more rapid recovery times. As with Mean- or Low- Streamflow, the salt
 393 intrusion moves up-estuary during the period of closure. However, once the gates are opened, the
 394 barotropic-forced depth-averaged outflow (with some modulation by the tides) quickly advects
 395 the salinity anomalies seaward (Figure 5). Hurricane Irene is an extreme case, with the highest
 396 river discharge at this area in the past 70 years washing salt almost entirely out of the Hudson
 397 past Manhattan (Ralston & Geyer, 2019). However, the overall trend toward lesser salt intrusion
 398 length changes and recovery time for higher streamflows suggests this is an endmember where
 399 there are lesser impacts on salinity, and therefore we did not run simulations for longer durations
 400 than the pre-existing 10-day Irene simulation of Orton et al. (2012). As noted in Chen et al.
 401 (2020), trapped river water rises high inside the harbor (Figure 5, red line), which would prevent
 402 longer-duration closures in compound floods, but here we simply demonstrate the resulting
 403 effects of 3-day and 5-day closures for the sake of symmetric comparison to Low- and Mean-
 404 Streamflow scenarios.



405

406 **Figure 5.** Hurricane Irene Open-Barrier scenario (panel a) and single (annual) 3-day Gate-
 407 Closure scenario (panel b) Spatio-temporal stratification plots. These show modeled salinity
 408 stratification ($\Delta S = S_{\text{bottom}} - S_{\text{surface}}$) along the thalweg (color shading), the length of the salt
 409 intrusion (white line), and water level at the Battery (red line) with an arbitrary scale. (panel c)
 410 The color shading represents the corresponding changes in salinity stratification (Gate-Closure
 411 scenario minus Open-Barrier scenario). The vertical dashed lines show the time of gate closure
 412 or reopening.

413 3.3 Stratification, intrusion and recovery time analyses

414 Gate closures eliminate the tidal mixing process, enabling significant increases in estuary
 415 stratification and salt intrusion length. In this section, we evaluate the salinity impacts from
 416 single gate closure scenarios and the recovery time after gate reopening, focusing on the Low-
 417 and Mean- Streamflow scenarios. The resulting salinity and stratification extremes are also
 418 compared to the historical variations arising only from natural forces.

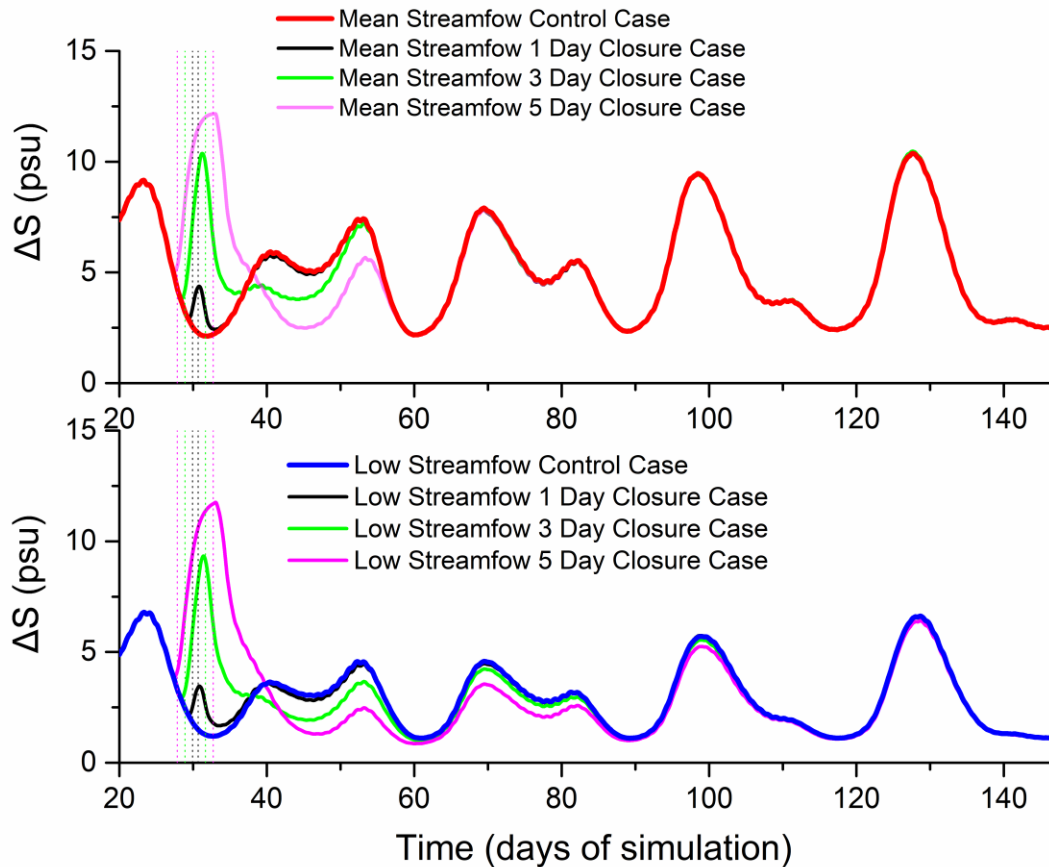
419 The estuary spatial-average salinity stratification (Figure 6) shows a significant but temporary
 420 increase after gate closure. A 3-day (or longer) gate closure can cause comparable or even larger
 421 changes of the salinity stratification than its variation between the perigean spring tide
 422 (simulation day 119) and apogean neap tide (day 126).

423 After the gates reopen, the vertical mixing is rapidly restored, though the stratification decreases
 424 more slowly than it increased during closure. The excess spatial-average stratification behind the
 425 barrier domain caused by gate closure disappears within days, though the excess stratification
 426 near the head of the salt intrusion takes longer to disappear. The excess stratification disappears
 427 along the salt wedge from the seaward end to the river upstream (shown in the bottom two panels
 428 in Figure 4).

429 After the rapid mixing out of excess stratification, much of the estuary has a lower stratification
 430 than that of the Control simulation (Figure 6 and the dark blue shading in the bottom two panels
 431 e,f in Figure 4). These negative anomalies in stratification will last until the recovery of the
 432 estuary length because during this time the tidal mixing is recovered but its salt intrusion length
 433 is still longer than that of the Control. A longer salt intrusion length and resulting weaker along-
 434 estuary salinity (and density) gradient results in a weaker baroclinic force. Given the same
 435 barotropic forcing as control, a weaker baroclinic force results in reduced subtidal stratification
 436 generation below that of the Control (Geyer & MacCready, 2014). As the salt intrusion length
 437 decreases, the estuary salinity stratification gradually asymptotes back to the Control.

438 During recovery from gate closure, the simulation results suggest that the salt wedge can get cut
 439 off (e.g., Panel 3 in Figure 3). The Tappan Zee and Haverstraw regions of the estuary (25-40 km)
 440 can have saline, stratified water, and an area off Manhattan centered near George Washington
 441 Bridge (GWB) can be much more well-mixed and have lower salinity water. This could arise due
 442 to stronger tidal currents and associated mixing in the narrower areas from 10-20 km, compared
 443 to weaker currents in the wider areas from 25-40 km. The vertical mixing from 10-20 km could
 444 also be caused by convergence and particularly strong tidal currents around a constriction at
 445 GWB (e.g., Chant & Wilson, 1997).

446



447

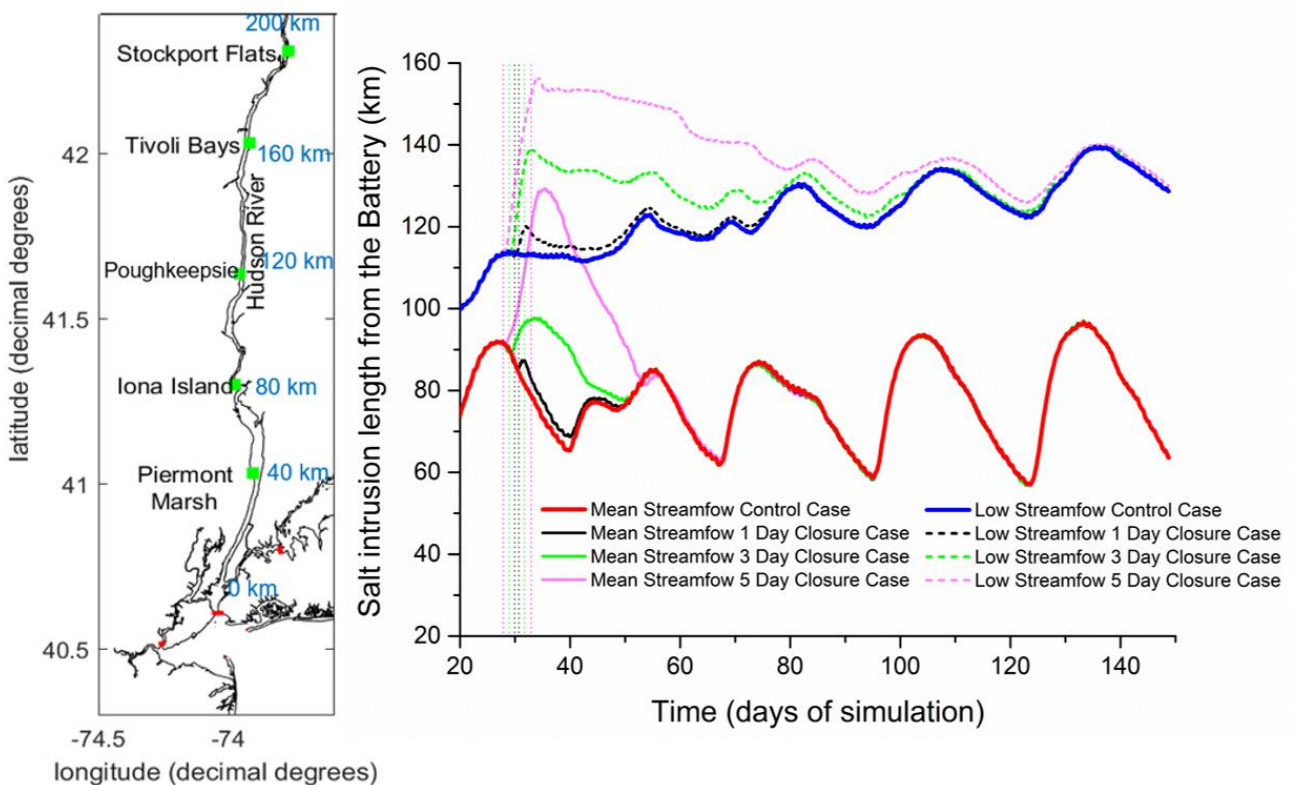
448 **Figure 6.** Modeled sub-tidal spatial-average estuary salinity stratification under Mean-
 449 Streamflow (top) and Low-Streamflow (bottom). Gate closure times are approximately day 29.9,
 450 28.9, 27.9 and gate reopening times are approximately day 30.7, 31.7, 32.7, for 1, 3, and 5 day
 451 “Gate-Closure” scenarios, respectively. The vertical dashed lines show the time of gate closure
 452 or reopening.

453 Figure 7 shows the temporal variation of sub-tidal salt intrusion length along the thalweg. When
 454 the barrier gates are closed, it eliminates tidal mixing in the estuary and the salt front location
 455 will move rapidly upriver, driven by the baroclinic force. A long duration gate closure (3-day or
 456 longer) will cause a significant increase in salt intrusion length which is similar to the annual
 457 maximum intrusion induced by an apogean neap tide. However, a short-duration gate closure
 458 (e.g., 1 day) only causes a sub-tidal salt intrusion increment of less than 10 km (Figure 7).

459 The salt intrusion can go further northward to Poughkeepsie and potentially affect its water
 460 supply (as described in Section 3.2.1) in the scenarios with 5-day closure under Mean-
 461 Streamflow and 3- or 5-day closure under Low-Streamflow (Figure 7). Moreover, the maximum
 462 salt intrusion is a few kilometers longer than the sub-tidal salt intrusion length shown, due to the
 463 semidiurnal tidal variations of about 5-10 km.

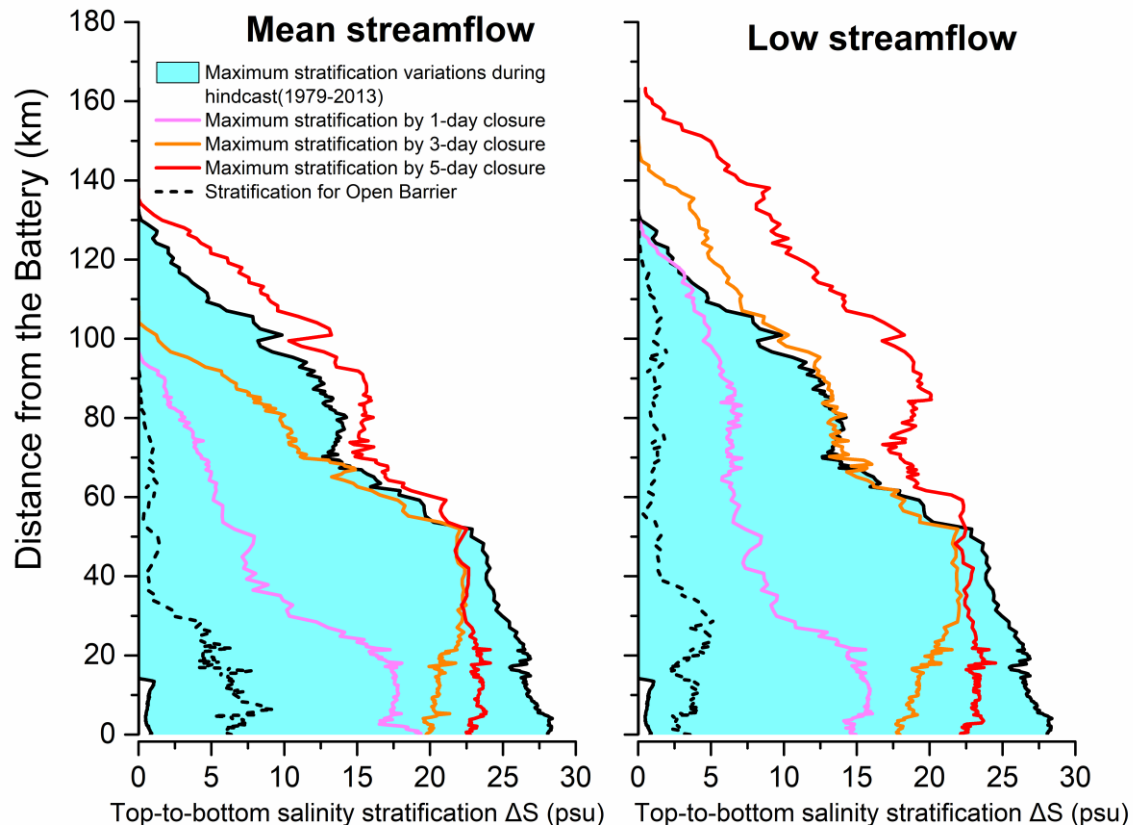
464 The salt intrusion advance speed during closure under Low-Streamflow is slightly higher than
 465 that for Mean-Streamflow, which causes it to have a longer salt intrusion increment (the
 466 immediate increase due to closure). More importantly, under low streamflow conditions, there is
 467 a combined effect of the salt intrusion from both gate closure and the dry conditions, which
 468 could cause salt intrusion extremes for the estuary. Figure 7 shows the maximum sub-tidal salt
 469 intrusion length can almost reach 158 km away from the Battery (around the Tivoli Bay wetland
 470 reserve site) with a 5-day closure under Low-Streamflow conditions. A gradual salt intrusion
 471 increase continues to occur throughout the simulation, driven by a progression toward an
 472 apogean neap tide and the extended period of constant low discharge. However, this has a
 473 negligible effect on the recovery time evaluations where we evaluate the difference from a
 474 control simulation and an experiment.

475 Recovery of the salt intrusion to normal after gate re-opening is slow under low streamflow,
 476 significantly slower than under Mean-Streamflow. The monthly closure simulation results for
 477 Low-Streamflow conditions (e.g., Figure S2-o or S2-p) show that repetitive high-frequency
 478 closures would enable the salt intrusion length to consecutively increase (relative to control)
 479 because there is insufficient time for recovery.
 480



481
 482 **Figure 7.** Modeled sub-tidal salt intrusion length under various scenarios (right). The salt
 483 intrusion length is defined as the distance of the 1-psu thalweg bottom salinity from the Battery,
 484 with distances shown in blue on the Hudson River estuary map (left). The vertical dashed lines
 485 show the time of gate closure or reopening.

486 Figure 8 compares the salt stratification conditions caused by the gate closures to the range of
 487 stratification variation from 1979-2013 based on a well-validated hindcast simulation (Georgas,
 488 Yin, et al., 2016). This gives a clear picture of how extremes of stratification and saltwater
 489 intrusion caused by gate closures along the estuary compare to historic maximum variations
 490 under natural forcings (e.g., tide, streamflow). The salt stratification along the upper estuary can
 491 be greater than its 35-year maximum values from effects of a single 5-day closure under Mean-
 492 Streamflow or single 3- or 5-day closure under Low-Streamflow scenarios. The salinity regime
 493 also exceeds its 35-year maximum for these cases. Moreover, these closures all occur during
 494 spring tide in the simulations, when the estuary has relatively low stratification. Gate closures at
 495 other phases of the spring-neap cycle can cause stronger stratification and longer salt intrusion
 496 conditions along the estuary, as demonstrated in SM section (Text S2.2). After a 1-day gate
 497 closure, the estuary does not become strongly stratified. Only upstream areas within 30 km from
 498 the Battery have the salt stratification above 10 psu (Figure 8), which is lower than its
 499 stratification during the neap tide. While 1-day gate closures can cause abrupt physical changes,
 500 the effects on salt intrusion and stratification are not extreme (Figure 6-7).



501

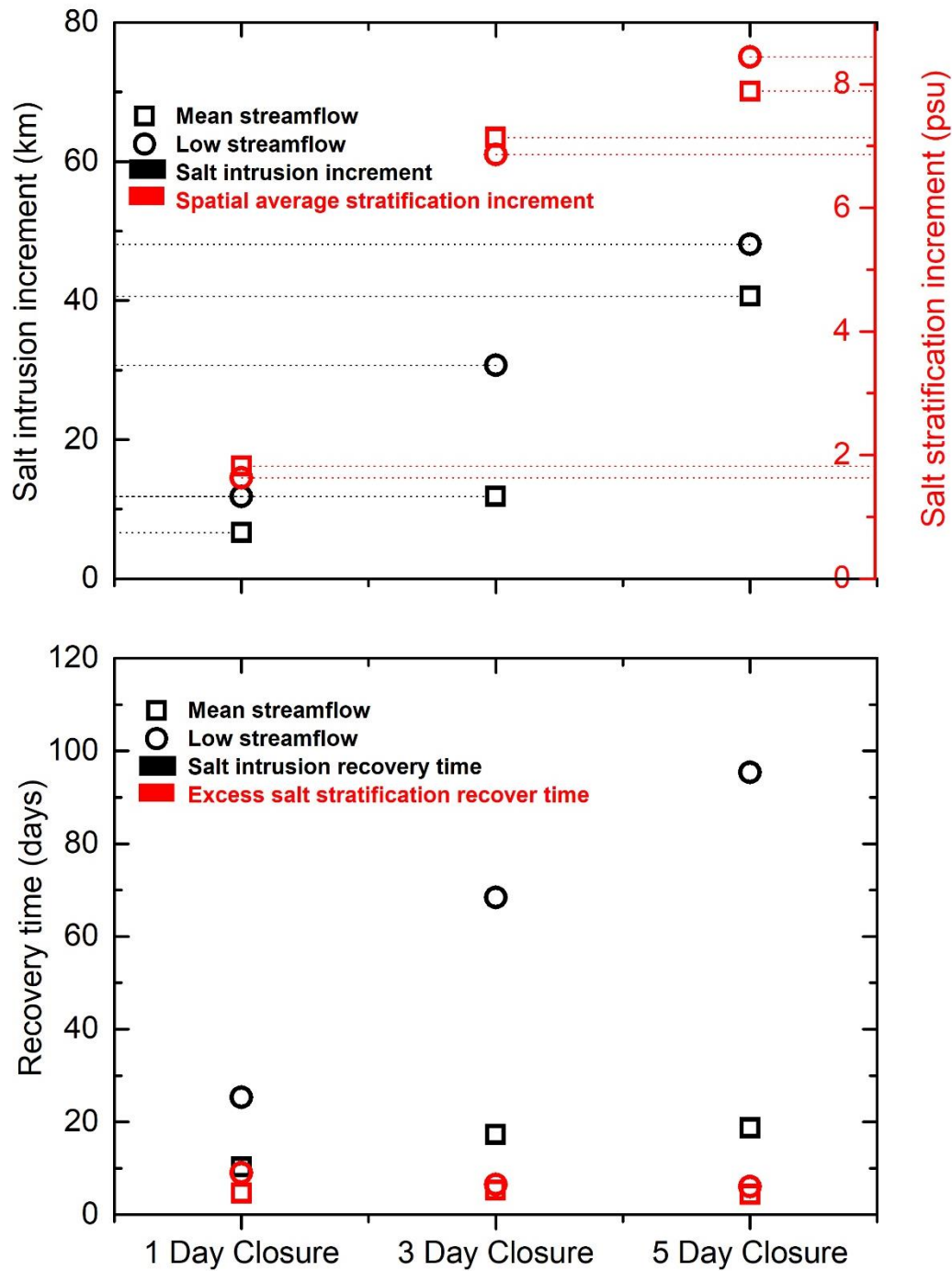
502 **Figure 8.** Modeled salinity stratification along the Hudson River thalweg under Mean-
 503 Streamflow (left) and Low- Streamflow (right). Color shading in blue is the maximum
 504 stratification variations over a 35-year hindcast. The red, orange and pink color lines are the
 505 maximum stratification from single (annual) Gate-Closure simulation. While not shown, the
 506 maximum salt intrusion length of 127 km is approximately 3 km below (seaward of) the tip of

507 the blue shading ($\Delta S \sim 0$). The salt stratification for each open-barrier control scenario (dashed
508 lines) at the time of the peak is shown (3-day closure peak) for comparison.

509 The increment of the estuary salt stratification from gate closure increases asymptotically with
510 closure duration and it is not sensitive to streamflow (Figure 9). After 3-day closure, certain
511 locations along the Hudson (20-60 km) can increase to an extreme stratification condition above
512 20 psu. The asymptotic behavior arises because a longer gate closure duration cannot make these
513 areas much more stratified, given that 25 psu is the maximum salinity in the estuary and no
514 saltwater is being added to the system during closure. The salt intrusion increment is sensitive to
515 the streamflow. Gate closures that occur under low streamflow will cause a longer increment
516 than under mean streamflow (Figure 9). The increment is almost linearly proportional to the
517 closure duration under low streamflow.

518 The salt intrusion recovery time is highly sensitive to the streamflow (Figure 9), as the speed for
519 the salt front to move seaward is quite different with various streamflow conditions shown in
520 Figure 7. Low streamflow can significantly extend the salt intrusion recovery time. The excess
521 salt stratification will recover within days after gate closure, which is significantly faster than the
522 salt intrusion length. The excess salt stratification recovery time is not sensitive to the gate
523 closure duration and streamflow condition.

524



525

526 **Figure 9.** Modeled salt intrusion or stratification increment (top) and their recovery times
 527 (bottom) versus gate closure durations under Mean- or Low-Streamflow. The legends show the
 528 meaning of the different shapes and colors.

529 4 Discussion

530 Our results for the Hudson River estuary show that short-duration surge barrier closures and
 531 closures under mean or higher streamflow would have a limited impact on saltwater intrusion

532 and stratification and a short recovery time well below one month. However, longer gate closure
533 durations (3 days or longer) could temporarily increase the salt intrusion and stratification
534 beyond the maxima in a 34-year hindcast (modeled with streamflow, tide, meteorology inputs).
535 Also, results show that monthly closures in dry periods could lead to durable changes to estuary
536 physical conditions, since one month is not sufficient time for recovery.

537 The salinity, salt intrusion length and stratification are critical physical parameters associated
538 with the estuarine environment, as well as up-estuary wetland habitat and freshwater resources.
539 Increases in stratification can reduce the vertical mixing, then weaken the water exchange, which
540 will affect the water quality by increasing residence time and potentially increasing the tendency
541 toward eutrophication, hypoxia (Paerl et al., 1998) and harmful algal blooms (Cousins et al.,
542 2010). For a tidal river estuary such as the Hudson, the extended salt intrusion can threaten the
543 freshwater supply at upstream locations (Hoagland et al., 2020), and increases in salinity can
544 threaten freshwater marshes and other vegetation (de Leeuw et al., 1994).

545 In the context of the USACE HAT study and barrier systems being studied that would affect the
546 Hudson, smaller Auxiliary Flow gates (46 m wide) could be temporarily opened during low tides
547 during a long-duration flood event (B. Wisemiller, USACE, pers. comm., 2021). This would
548 allow elevated water levels from river streamflows to escape and could feasibly enable some
549 tidally driven mixing within the estuary. However, if the much wider Navigational Gates were
550 not also opened, the influence of this pulsing on tidal propagation and mixing in the estuary is
551 likely small given that currents are flowing strongly outward at low tide. Moreover, tide
552 propagation into the estuary is very limited when only a small gated flow area of the barrier is
553 opened (Orton & Ralston, 2018). It is not clear how this could change the gate closure effects
554 and recovery, and an extremely high-resolution modeling study would be needed to simulate
555 these auxiliary flow gates and assess these specific management considerations.

556 Salinity recovery time in all our simulations is less than 100 days, which indicates that annual or
557 less frequent closures would allow for recovery between closures. The management plan initially
558 presented for the HAT Study would involve surge barrier closures for 2-year return period events
559 or worse (USACE, 2019, p69). This would be a rational management plan for the surge barrier
560 system, with respect to recoverability of salinity conditions. Other recent surge barrier studies
561 have similarly recommended infrequent closures and management planning so that SLR doesn't
562 raise the closure frequency (e.g., USACE, 2020b, 2021a).

563 However, a new HAT Study report includes no limits on closure frequency, leaving it open to
564 further study (USACE, 2022, p220). If the gate is closed more frequently in response to SLR, as
565 was demonstrated as a possible future scenario by Chen et al. (2020), monthly gate closures with
566 low streamflow will be problematic because the system needs more time to recover. For
567 example, with 0.6 m SLR, the gate closure frequency at the Hudson would increase from 0.15
568 times per year to 3 times per year. This would increase the likelihood of higher frequency
569 closures (e.g., monthly) and potential associated estuary aggregate impacts with consecutive salt
570 intrusion increasingly moving up the estuary (e.g., Figure S2-o or S2-p).

571 Our results are focused on modeling of one estuary and are based on several simplifying
572 assumptions to demonstrate the primary factors, processes and effects of surge barrier closures.
573 We focus on a long river-estuary, yet other types of estuaries can have different salinity

574 dynamics, as discussed below in Section 4.3. We use simplified constant Mean- and Low
575 Streamflow condition scenarios, whereas streamflow can vary in response to rain events and
576 snowmelt. We assume that the water depth is not changing and ignore the large uncertainties of
577 future SLR, geomorphic response, and dredging for shipping. We show in Supplementary Text
578 S2.1 how increased water depths can have similar effects to surge barriers and these results are
579 discussed below in Section 4.1 in the context of historical changes to the Hudson. We neglect
580 wind effects in the modeling, but we demonstrate that this is a secondary factor in a narrow
581 estuary like the Hudson (Text S2.4). Complexities of diffusion in the salt intrusion modeling
582 during gate closure are addressed through the sensitivity to the horizontal Prandtl number (Text
583 S2.3). Also, some modeling studies (e.g., Kärnä et al., 2015) have struggled to accurately
584 produce sharp salinity fronts in highly energetic estuaries due to numerical diffusion, and others
585 have shown how grid resolution can affect results (e.g., Ralston et al., 2017). The problem of
586 numerical diffusion could affect the results, but this is somewhat mitigated by the use of a
587 structured grid model like sECOM (e.g., Ralston et al., 2017). Moreover, in our study there are
588 low water speeds during barrier closures and relatively small salinity gradients around the salt
589 front. As a result, we expect numerical diffusion to have a limited effect on our results.
590 Nevertheless, numerical diffusion and resolution sensitivity studies would be useful in future
591 research.

592 Below in Section 4.1, we contextualize the surge barrier effects relative to future SLR, climate
593 change and historical dredging effects. In Section 4.2 we further discuss how the surge barrier
594 closure effects compare to normal estuary variations and SLR. In Section 4.3, we consider the
595 general applicability of the gate closure assessment approach taken here for other constructed or
596 proposed estuary surge barriers, and in Section 4.4, we synthesize our results with the estuary
597 dynamics literature to outline the critical factors governing recovery time from gate closure.

598 4.1 Combined effects from sea-level rise, dredging and climate change

599 Increasingly extreme salt intrusion effects may appear from the surge barrier protection coupled
600 with future SLR and dredging. First, SLR (or dredging) could increase the water depth and increase
601 the salt intrusion of an estuary. The salt intrusion effects of gate closure also are amplified by SLR
602 or dredging (Text S2.1). Moreover, SLR could cause there to be more frequent gate closures which
603 may not allow enough time for estuary conditions to recover, as noted above (Chen et al., 2020).
604 These cumulative effects could raise the frequency and intensity of salt intrusion changes for an
605 estuary, which will increase the risk of affecting the upstream freshwater resources.

606 The effect of SLR on estuary depths depends on whether increasing sedimentation raises the bed
607 level (e.g., Nichols, 1989), so areas with lower sediment delivery (e.g., New York Harbor;
608 Rodenburg & Ralston, 2017) are more likely to have water depth increases than areas replete with
609 sediment (e.g., the Hudson; Ralston et al., 2013). Predicting the future sedimentary response of
610 estuaries to SLR is a challenging problem for models (e.g., Baar et al., 2019). Furthermore, depths
611 are also often increased by dredging of major estuaries for shipping. For example, the channel
612 deepening on the Hudson River in the past 150 years increased the estuary salinity intrusion by
613 about 30% and increased the stratification by 5% to 30% depending on streamflow (Ralston &
614 Geyer, 2019).

615 Climate change can also affect the salt intrusion by altering future precipitation and the seasonal
616 hydrograph. Climate change has somewhat complex and competing effects on future streamflow,
617 causing both drying of the land due to increasing evaporation and intensified rainfall due to
618 increased atmospheric moisture. Globally, temperatures will become warmer which will increase
619 the drying of the land due to evaporation. Enhanced drought conditions may worsen surge barrier
620 effects due to lower streamflows and slower recovery times. However, the extreme events could
621 have increased rainfall, particularly for the Northeastern US (Horton et al., 2014), which could
622 result in increased storm-driven and mean streamflows. It is challenging to predict the streamflow
623 variations in the future. Overall, an important additional area of future research is that of the
624 combination of climate change, human interference and surge barrier effects on estuaries.

625 4.2 Context of surge barrier effects relative to normal estuary variations

626 The Hudson River estuary salt intrusion and stratification are typically controlled by tidal
627 amplitude and streamflow (Orton & Visbeck, 2009; Ralston et al., 2008). For example,
628 observation shows that the spring-neap tide modulation can cause about 30 km salinity intrusion
629 length variation (Ralston et al., 2008) and a ~15 psu mid-estuary salinity stratification variation
630 (Orton & Visbeck, 2009) for the Hudson River under a relatively stable moderate streamflow
631 condition. Streamflow variation can also strongly affect the salt intrusion length, as the salt
632 intrusion can be as short as 40 km from the Battery after an extreme spring freshet (Geyer et al.,
633 2001) and reach about 120 km after a severe summer drought (Bowen & Geyer, 2003).

634 The surge barrier system can bring similar magnitude perturbations to estuary conditions when
635 there are gate closures (Figure 9), but these occur more rapidly (Figure 4). Also, this
636 anthropogenic disturbance can work together with other natural forces and create more extreme
637 salinity spatial distributions than normally occur in an estuary (Figure 8).

638 4.3 Research framework (or metrics) recommendations for other estuary barrier 639 evaluations

640 In this research, we developed a computational modeling approach and set of metrics to assess
641 the potential physical estuary effects of storm surge barriers. Our analysis in this paper is based
642 on one widely-studied estuary, but similar research could be performed on a wide range of
643 estuary types. Our assessment approach focused on year-round open barrier effects, modeling
644 effects of barrier closures, assessing saltwater intrusion and stratification recovery times, and
645 comparing the changes to data on past historical variations.

646 Considering the broader range of estuary types characterized by Geyer and MacCready (2014)
647 with a freshwater Froude Number and Mixing Number parameter space, the Hudson has a
648 varying character from strongly stratified salt-wedge to partially-mixed estuary. In this regard,
649 our range of conditions represents a wide range of river-estuaries, but neglects relatively well-
650 mixed and only periodically stratified systems (e.g., San Francisco Bay, Tamar River, Willapa
651 Bay) and the bay-type and lagoonal estuary systems (e.g., Barnegat Bay, Narragansett Bay).
652 Our study captures the range of freshwater Froude numbers modestly well but does not span a
653 wide range of mixing numbers.

654 Estuaries with high populations vulnerable to storm surge flooding are both likely locations for
655 surge barrier construction and for pollution. The temporary and potential chronic changes
656 identified in this study, increased stratification and salt intrusion, can also reflect increases in
657 residence times that can worsen problems with hypoxia and pollution (e.g., Wurtsbaugh et al.,
658 2019). Thus, water (and nutrient and pollutant) residence times and potentially biogeochemical
659 modeling should be used to evaluate surge barrier effects in such systems (e.g., Marsooli et al.,
660 2018) to better understand these broader possible effects on the estuary environment and
661 ecosystems.

662 4.4 Controlling factors for estuary recovery time after closure

663 The response of stratification and salt intrusion to variations in river flow and tidal mixing has
664 been explored by many past studies (e.g., Kranenburg, 1986; MacCready & Geyer, 2010). The
665 length of the salt intrusion and the mean outflow velocity (due to streamflow) are the main
666 driving mechanisms that control the “estuary adjustment timescale” to a new equilibrium
667 (MacCready, 2007). With surge barrier closures, we are interested in the timescale to recover
668 back to a prior equilibrium after an abrupt perturbation (gate closure), but there is some
669 similarity to the estuary adjustment timescale and its dynamics, as shown by our results and
670 discussed below.

671 The closure duration is a primary factor influencing recovery time as it defines the magnitude of
672 the initial perturbation to the estuary conditions. The dense salty water on the bottom layer will
673 keep move upriver until the gate is reopened and the estuary tidal mixing restarts. Both long
674 duration flood events and multiple flood events in tandem could cause long gate closure
675 duration.

676 Our results indicate that streamflow is an important factor governing recovery time, similar to
677 the estuary adjustment timescale. During high river discharge like Irene (Section 3.3), there is no
678 salt intrusion increase. The salt intrusion length recovers much faster with Mean-Streamflow
679 than with Low-Streamflow. However, the rate of streamflow varies lot during a storm surge
680 flooding event or a tidal flooding event. So, the gate closure’s impact and its recovery time will
681 vary with different flood events depending on the streamflow conditions.

682 SLR can also affect the recovery time in an indirect way because it could cause more closures
683 due to tidal flooding that often occurs under low streamflow, non-storm conditions. It is not
684 uncommon for there to be 2-4 month periods with streamflows similar to our Low-Streamflow
685 scenario in summertime (Green Island Station 01358000; USGS, 2021). The most extreme long-
686 duration example was a drought period in 1995 when streamflow was below our “dry” value of
687 $150 \text{ m}^3/\text{s}$ for about 5 months with a mean of only $111 \text{ m}^3/\text{s}$. Normally, there is a low probability
688 to have repeated storm surge events with low streamflow conditions. However, if barrier closure
689 is managed by a constant water level threshold, instead of a constant return period, a growing
690 number of spring tide flood events will trigger the gate closure without storms (Chen et al.,
691 2020), which have a high probability to occur during periods of low streamflow.

692 Estuary length is another factor that affects the adjustment timescale, and due to the dynamical
693 similarity of recovery from barrier closures, likely also the estuary recovery time. Estuaries with
694 a longer estuary length (e.g., MacCready, 2007) or with a temporarily longer length (e.g.,

695 Lerczak et al., 2009) could slow its estuary response time to estuary physical changes. For
696 example, SLR (Tabak et al., 2016), channel dredging (Ralston & Geyer, 2019) or construction of
697 fixed surge barrier infrastructure (Orton & Ralston, 2018) can all extend the mean salt intrusion
698 length of the Hudson Estuary, which will increase the recovery time from gate closure effects as
699 well. Given the large range in estuary lengths with consideration of surge barrier construction
700 (e.g., Boston Harbor estuary with a shorter estuary length and Chesapeake Bay estuary with
701 longer estuary length; Du et al., 2017; Kirshen et al., 2020), the estuary recovery timescale from
702 gate closure will likely also depend on their estuary length.

703 **5 Conclusions**

704 In this study, we analyze the estuary effects of storm surge barriers, in particular gate closures,
705 on estuarine salt intrusion and stratification which have not been studied in the past academic
706 research. We develop a transferable framework to investigate the barriers closure effects on
707 estuary conditions considering control factors including closure frequency, duration and
708 streamflow conditions. Our research focuses on a narrow partially mixed estuary where wind
709 effects are secondary, and it would be worthwhile to perform similar research on other types of
710 estuaries with proposed surge barriers (e.g., lagoonal estuaries or wide estuaries). Our approach
711 here is to use simplified forcing scenarios, but future work could also apply full, variable forcing
712 with multi-year simulations.

713 The results for the Hudson River estuary indicate that an episodic gate closure event could cause
714 significantly larger but more temporary physical changes compared with the open barrier effects.
715 Gate closure causes rapid increases in stratification and salt intrusion length with the
716 latter increment proportional to the closure duration. So, a short-duration closure has limited
717 estuary impact. However, for 3-day duration closures, the estuary length experiencing unusually
718 high stratification values (over 20 psu) rises to equal the maximum length during 1979-2013 (52
719 km). For low or mean river discharge, 3 days closures can also lead to a 14-30 km excursion of
720 the salt intrusion up the estuary (an 18-40% increase). This can lead to conditions of salt
721 intrusion and stratification beyond their maxima over the past several decades, especially during
722 a low streamflow condition. If the surge barrier closures are not managed to avoid these extreme
723 conditions, they could threaten upstream municipal water supplies, and they could also affect the
724 estuary environment beyond these physical variables (e.g., estuary hypoxia, sediment trapping,
725 floodplain vegetation).

726 Increases in stratification are rapidly mixed out within days after gates reopen, and negative
727 anomalies in stratification last for a longer period. However, recovery time of salt intrusion to
728 normal is strongly dependent on streamflow, with the longest recovery times of well over one
729 month (but far less than one year) under low flow conditions. Monthly closures in dry periods
730 could lead to durable changes to estuary physical conditions. A biannual average gate closure
731 frequency, as initially proposed for the prospective surge barrier alternatives in the HAT Study,
732 would allow for physical recovery for the Hudson River estuary.

733 More broadly, we summarize the controls on gate closure recovery time that may have
734 implications on the consideration of surge barriers for flood risk reduction in other estuaries.
735 Long-duration closures lead to extended recovery times, as a longer closure duration creates a
736 larger initial perturbation to the estuary. A longer estuary length results from a long-duration

737 closure, then also slows the recovery time due to weakened longitudinal salinity gradient. The
 738 river discharge is also a primary controlling factor in limiting the duration of any extension of the
 739 salt intrusion. Gate closures during low streamflow situations need significantly longer recovery
 740 time.

741 The physical influences of open storm surge barriers and more acute changes when they are
 742 closed could lead to long-term changes to estuaries and their habitats. Our results show similar
 743 effects as those arising from SLR, climate warming and dredging in estuaries (e.g., Najjar et al.,
 744 2010; Ralston & Geyer, 2019; Rice et al., 2012). Therefore, an important continued area of
 745 research is on the combination of climate change and surge barrier effects on the physical and
 746 ecological conditions of estuaries.

747 Acknowledgments

748 This research was funded by the New York State Energy Research and Development Authority
 749 (NYSERDA; agreement 145583) and the NOAA Regional Integrated Sciences and Assessments
 750 (RISA) program project Consortium for Climate Risk in the Urban Northeast (CCRUN; awards
 751 NA15OAR4310147 and NA21OAR4310313). The authors gratefully acknowledge James
 752 Fitzpatrick and Nicholas Kim (HDR, Inc.) for providing their source model code used in their
 753 prior project. The authors would like to thank three anonymous reviewers and associate editor
 754 for helping to improve the paper. We thank the constructive comments from David Ralston
 755 (WHOI) and Sarah Fernald (NOAA Hudson River National Estuarine Research Reserve and the
 756 New York State Energy Research and Development Authority). The authors are also grateful to
 757 Jay Titlow of Weatherflow for providing the wind observations for this research.

758 Open Research

759 The model inputs, bathymetric data and selected model results are available at (Chen, Z. &
 760 Orton, P. 2022).

761

762 References

- 763 Akter, R., Asik, T. Z., Sakib, M., Akter, M., Sakib, M. N., Al Azad, A. S. M. A., et al. (2019). The Dominant
 764 Climate Change Event for Salinity Intrusion in the GBM Delta. *Climate*, 7(5), 69.
 765 <https://www.mdpi.com/2225-1154/7/5/69>
 766 Baar, A., Boechat Albernaz, M., Van Dijk, W., & Kleinhans, M. (2019). Critical dependence of morphodynamic
 767 models of fluvial and tidal systems on empirical downslope sediment transport. *Nature communications*,
 768 10(1), 1-12.
 769 Bakker, C., Herman, P., & Vink, M. (1990). Changes in seasonal succession of phytoplankton induced by the storm-
 770 surge barrier in the Oosterschelde (SW Netherlands). *Journal of Plankton Research*, 12(5), 947-972.
 771 Bowen, M., & Geyer, W. (2003). Salt Transport and the Time-dependent Salt Balance of a Partially Stratified
 772 Estuary. *Journal of Geophysical Research*, 108.
 773 Chant, R., & Wilson, R. (1997). Secondary circulation in a highly stratified estuary. *Journal of Geophysical*
 774 *Research*, 1022, 23207-23216.
 775 Chen, Z., Orton, P. M., & Wahl, T. (2020). Storm Surge Barrier Protection in an Era of Accelerating Sea Level Rise:
 776 Quantifying Closure Frequency, Duration and Trapped River Flooding. *Journal of Marine Science and*
 777 *Engineering*, 8(9), 725.

- 778 Chen, Z., & Orton P. (2022), "Chen_Orton_WRR_DATA", Mendeley Data, V1, [The bathymetric data, model
779 inputs and selected model results for estuary modeling from storm surge barrier closures]. doi:
780 10.17632/v9y9drdxbf.1.
- 781 Chen, S.-N., & Sanford, L. P. (2009). Axial Wind Effects on Stratification and Longitudinal Salt Transport in an
782 Idealized, Partially Mixed Estuary. *Journal of Physical Oceanography*, 39(8), 1905-1920.
783 <http://dx.doi.org/10.1175%2F2009JPO4016.1>
- 784 Cloern, J. E., Knowles, N., Brown, L. R., Cayan, D., Dettinger, M. D., Morgan, T. L., et al. (2011). Projected
785 Evolution of California's San Francisco Bay-Delta-River System in a Century of Climate Change. *Plos*
786 *One*, 6(9), e24465. <https://doi.org/10.1371/journal.pone.0024465>
- 787 Cottingham, A., Huang, P., Hipsey, M. R., Hall, N. G., Ashworth, E., Williams, J., & Potter, I. C. (2018). Growth,
788 condition, and maturity schedules of an estuarine fish species change in estuaries following increased
789 hypoxia due to climate change. *Ecology and Evolution*, 8(14), 7111-7130.
790 <https://onlinelibrary.wiley.com/doi/abs/10.1002/ece3.4236>
- 791 Cousins, M., Stacey, M. T., & Drake, J. L. (2010). Effects of seasonal stratification on turbulent mixing in a
792 hypereutrophic coastal lagoon. *Limnology and Oceanography*, 55(1), 172-186.
793 <https://aslopubs.onlinelibrary.wiley.com/doi/abs/10.4319/lo.2010.55.1.0172>
- 794 de Leeuw, J., Apon, L. P., Herman, P. M., de Munck, W., & Beetsink, W. G. (1994). *The response of salt marsh*
795 *vegetation to tidal reduction caused by the Oosterschelde storm-surge barrier*: Springer.
- 796 Deltacommissie. (2009). *Working together with water: A living land builds for its future. Findings of the*
797 *Deltacommissie 2008, summary and conclusions*: Hollandia Printing.
- 798 Du, J., Shen, J., Bilkovic, D. M., Hershner, C. H., & Sisson, M. (2017). A numerical modeling approach to predict
799 the effect of a storm surge barrier on hydrodynamics and long-term transport processes in a partially mixed
800 estuary. *Estuaries and Coasts*, 40(2), 387-403.
- 801 Du, J., Shen, J., Park, K., Wang, Y. P., & Yu, X. (2018). Worsened physical condition due to climate change
802 contributes to the increasing hypoxia in Chesapeake Bay. *Science of The Total Environment*, 630, 707-717.
803 <https://www.sciencedirect.com/science/article/pii/S004896971830665X>
- 804 Edson, J. B., Jampana, V., Weller, R. A., Bigorre, S. P., Plueddemann, A. J., Fairall, C. W., et al. (2013). On the
805 Exchange of Momentum over the Open Ocean. *Journal of Physical Oceanography*, 43(8), 1589-1610.
806 <https://journals.ametsoc.org/view/journals/phoc/43/8/jpo-d-12-0173.1.xml>
- 807 Georgas, N., Blumberg, A., Herrington, T., Wakeman, T., Saleh, F., Runnels, D., et al. (2016). The Stevens Flood
808 Advisory System: Operational H3e Flood Forecasts For The Greater New York/New Jersey Metropolitan
809 Region. *International Journal of Safety and Security Engineering*, 6(3), 648-662.
- 810 Georgas, N., & Blumberg, A. F. (2010, 4-6 November). *Establishing Confidence in Marine Forecast Systems: The*
811 *Design and Skill Assessment of the New York Harbor Observation and Prediction System, Version 3*
812 *(NYHOPS v3)*. Paper presented at the Eleventh International Conference in Estuarine and Coastal Modeling
813 (ECM11), Seattle, Washington, USA.
- 814 Georgas, N., & Blumberg, A. F. (2011). *sECOM and its NYHOPS v3 App. A high-fidelity, general, robust,*
815 *automated, operational forecast model applied to the NY/NJ Harbor Estuary and its surroundings*. Paper
816 presented at the Chesapeake Community Modeling Program, Edgewater, MD.
- 817 Georgas, N., Yin, L., Jiang, Y., Wang, Y., Howell, P., Saba, V., et al. (2016). An Open-Access, Multi-Decadal,
818 Three-Dimensional, Hydrodynamic Hindcast Dataset for the Long Island Sound and New York/New Jersey
819 Harbor Estuaries. *Journal of Marine Science and Engineering*, 4(48).
- 820 Geyer, W. R., & MacCready, P. (2014). The estuarine circulation. *Annual Review of Fluid Mechanics*, 46.
- 821 Geyer, W. R., Woodruff, J., & Traykovski, P. (2001). Sediment transport and trapping in the Hudson River Estuary.
822 *Estuaries and Coasts*, 24(5), 670-679.
- 823 Georgas, N., Yin, L., Jiang, Y., Wang, Y., Howell, P., Saba, V., et al. (2016). An Open-Access, Multi-Decadal,
824 Three-Dimensional, Hydrodynamic Hindcast Dataset for the Long Island Sound and New York/New Jersey
825 Harbor Estuaries. *Journal of Marine Science and Engineering*, 4(48).
- 826 Gong, W., Lin, Z., Chen, Y., Chen, Z., & Zhang, H. (2018). Effect of winds and waves on salt intrusion in the Pearl
827 River estuary. *Ocean Sci.*, 14(1), 139-159. <https://os.copernicus.org/articles/14/139/2018/>
- 828 Gornitz, V., Oppenheimer, M., Kopp, R., Horton, R., Bader, D., Orton, P., & Rosenzweig, C. (2020). Enhancing
829 New York City's Resilience to Sea Level Rise and Increased Coastal Flooding. *Urban Climate*, 33, 100654.
- 830 Hoagland, P., Beet, A. R., Ralston, D. K., Parsons, G. R., Shirazi, Y. A., & Carr, E. (2020). *Salinity Intrusion in a*
831 *Modified River-Estuary System: An Integrated Modeling Framework for Source-to-Sea Management*. Paper
832 presented at the Frontiers in Marine Science.

- 833 Horton, R., Yohe, G., Easterling, W., Kates, R., Ruth, M., Sussman, E., et al. (2014). Ch. 16: Northeast. In J. M.
834 Melillo, T. C. Richmond, & G. W. Yohe (Eds.), *Climate Change Impacts in the United States: The Third*
835 *National Climate Assessment* (pp. 371-395): U.S. Global Change Research Program.
- 836 Jordi, A., Georgas, N., Blumberg, A., Yin, L., Chen, Z., Wang, Y., et al. (2019). A next-generation coastal ocean
837 operational system: Probabilistic flood forecasting at street scale. *Bulletin of the American Meteorological*
838 *Society*, 100(1), 41-54.
- 839 Kärnä, T., Baptista, A. M., Lopez, J. E., Turner, P. J., McNeil, C., & Sanford, T. B. (2015). Numerical modeling of
840 circulation in high-energy estuaries: A Columbia River estuary benchmark. *Ocean modelling*, 88, 54-71.
841 <https://www.sciencedirect.com/science/article/pii/S1463500315000037>
- 842 Kirshen, P., Borrelli, M., Byrnes, J., Chen, R., Lockwood, L., Watson, C., et al. (2020). Integrated assessment of
843 storm surge barrier systems under present and future climates and comparison to alternatives: a case study
844 of Boston, USA. *Climatic Change*, 162(2), 445-464. <https://doi.org/10.1007/s10584-020-02781-8>
- 845 Kirshen, P., Thurson, K., McMann, B., Foster, C., Sprague, H., Roberts, H., et al. (2018). *Feasibility of Harbor-wide*
846 *Barrier Systems: Preliminary Analysis for Boston Harbor*. Retrieved from Sustainable Solutions Lab,
847 University of Massachusetts Boston:
- 848 Kopp, R. E., Horton, R. M., Little, C. M., Mitrovica, J. X., Oppenheimer, M., Rasmussen, D., et al. (2014).
849 Probabilistic 21st and 22nd century sea-level projections at a global network of tide-gauge sites. *Earth's*
850 *Future*, 2(8), 383-406.
- 851 Kranenburg, C. (1986). A Time Scale for Long-Term Salt Intrusion in Well-Mixed Estuaries. *Journal of Physical*
852 *Oceanography*, 16(7), 1329-1331. https://journals.ametsoc.org/view/journals/phoc/16/7/1520-0485_1986_016_1329_atstft_2_0_co_2.xml
- 853 Lavery, S., & Donovan, B. (2005). Flood risk management in the Thames Estuary looking ahead 100 years. *Philos*
854 *Trans A Math Phys Eng Sci*, 363(1831), 1455-1474.
- 855 Lerczak, J. A., Geyer, W. R., & Ralston, D. K. (2009). The Temporal Response of the Length of a Partially
856 Stratified Estuary to Changes in River Flow and Tidal Amplitude. *Journal of Physical Oceanography*,
857 39(4), 915-933. <https://journals.ametsoc.org/view/journals/phoc/39/4/2008jpo3933.1.xml>
- 858 Leuven, J. R. F. W., Pierik, H. J., Vegt, M. v. d., Bouma, T. J., & Kleinhans, M. G. (2019). Sea-level-rise-induced
859 threats depend on the size of tide-influenced estuaries worldwide. *Nature Climate Change*, 9(12), 986-992.
860 <https://doi.org/10.1038/s41558-019-0608-4>
- 861 Levinton, J. S., Levinton, J. S., & Waldman, J. R. (2006). *The Hudson River Estuary*: Cambridge University Press.
- 862 Lin, N., Emanuel, K., Oppenheimer, M., & Vanmarcke, E. (2012). Physically based assessment of hurricane surge
863 threat under climate change. *Nature Climate Change*, 2(6), 462-467.
- 864 Lerczak, J. A., Geyer, W. R., & Ralston, D. K. (2009). The Temporal Response of the Length of a Partially
865 Stratified Estuary to Changes in River Flow and Tidal Amplitude. *Journal of Physical Oceanography*,
866 39(4), 915-933. <https://journals.ametsoc.org/view/journals/phoc/39/4/2008jpo3933.1.xml>
- 867 MacCready, P. (2007). Estuarine adjustment. *Journal of Physical Oceanography*, 37(8), 2133-2145.
- 868 MacCready, P., & Geyer, W. R. (2010). Advances in Estuarine Physics. *Annual Review of Marine Science*, 2(1), 35-
869 58. <https://www.annualreviews.org/doi/abs/10.1146/annurev-marine-120308-081015>
- 870 Marsooli, R., Lin, N., Emanuel, K., & Feng, K. (2019). Climate change exacerbates hurricane flood hazards along
871 US Atlantic and Gulf Coasts in spatially varying patterns. *Nature communications*, 10(1), 3785.
872 <https://doi.org/10.1038/s41467-019-11755-z>
- 873 Marsooli, R., Orton, P. M., Fitzpatrick, J., & Smith, H. (2018). Residence time of a highly urbanized estuary:
874 Jamaica Bay, New York. *Journal of Marine Science and Engineering*, 6(44).
- 875 Mooyaart, L., & Jonkman, S. N. (2017). Overview and Design Considerations of Storm Surge Barriers. *Journal of*
876 *Waterway, Port, Coastal, and Ocean Engineering*, 143(4), 06017001.
- 877 Najjar, R. G., Pyke, C. R., Adams, M. B., Breitburg, D., Hershner, C., Kemp, M., et al. (2010). Potential climate-
878 change impacts on the Chesapeake Bay. *Estuarine, Coastal and Shelf Science*, 86(1), 1-20.
- 879 National Research Council. (2014). *Reducing Coastal Risks on the East and Gulf Coasts*. Washington DC: The
880 National Academies Press.
- 881 Ni, W., Li, M., Ross, A. C., & Najjar, R. G. (2019). Large Projected Decline in Dissolved Oxygen in a Eutrophic
882 Estuary Due to Climate Change. *Journal of Geophysical Research: Oceans*, 124(11), 8271-8289.
883 <https://agupubs.onlinelibrary.wiley.com/doi/abs/10.1029/2019JC015274>
- 884 Nichols, M. M. (1989). Sediment accumulation rates and relative sea-level rise in lagoons. *Marine Geology*, 88(3-4),
885 201-219.
- 886 NYC-DEP. (2016). *Jamaica Bay Tidal Barrier Water Quality Modeling Analysis*, New York City Department of
887 *Environmental Protection, prepared by HDR, Inc.* New York, New York.
- 888

- 889 Orton, P., Georgas, N., Blumberg, A., & Pullen, J. (2012). Detailed modeling of recent severe storm tides in
 890 estuaries of the New York City region. *Journal of Geophysical Research*, 117, C09030.
- 891 Orton, P., Hall, T. M., Talke, S., Blumberg, A. F., Georgas, N., & Vinogradov, S. (2016). A Validated Tropical-
 892 Extratropical Flood Hazard Assessment for New York Harbor. *Journal of Geophysical Research*, 121.
- 893 Orton, P., Lin, N., Gornitz, V., Colle, B., Booth, J., Feng, K., et al. (2019). New York City Panel on Climate Change
 894 2019 Report Chapter 4: Coastal Flooding. *Annals of the New York Academy of Sciences*, 1439, 95-114.
- 895 Orton, P., & Ralston, D. (2018). Preliminary evaluation of the physical influences of storm surge barriers on the
 896 Hudson River estuary. Report to the Hudson River Foundation, 81pp. In.
- 897 Orton, P., Ralston, D., Prooijen, B., Secor, D., Ganju, N. K., Chen, Z., et al. (2022). Increased Utilization of Storm
 898 Surge Barriers: A Research Agenda on Estuary Impacts. (submitted). *Earth's Future*.
- 899 Orton, P., Sanderson, E. W., Talke, S. A., Giampieri, M., & MacManus, K. (2020). Storm tide amplification and
 900 habitat changes due to urbanization of a lagoonal estuary. *Nat. Hazards Earth Syst. Sci.*, 20(9), 2415-2432.
 901 <https://nhess.copernicus.org/articles/20/2415/2020/>
- 902 Orton, P., Vinogradov, S., Georgas, N., Blumberg, A., Lin, N., Gornitz, V., et al. (2015). New York City Panel on
 903 Climate Change 2015 report chapter 4: Dynamic coastal flood modeling. *Annals of the New York Academy*
 904 *of Sciences*, 1336(1), 56-66.
- 905 Orton, P., & Visbeck, M. (2009). Variability of internally generated turbulence in an estuary, from 100 days of
 906 continuous observations. *Continental Shelf Research*, 29(1), 61-77.
 907 <http://www.sciencedirect.com/science/article/B6VBJ-4PG873K-1/2/a7ae4cdb68706dc155bd736a2eae01b2>
- 908 Paerl, H., Pinckney, J., Fear, J., & Peierls, B. (1998). Ecosystem Responses to Internal and Watershed Organic
 909 Matter Loading: Consequences for Hypoxia in the Eutrophying Neuse River Estuary, North Carolina, USA.
 910 *Marine Ecology-progress Series - MAR ECOL-PROGR SER*, 166.
- 911 Ralston, D. K. (2022). Impacts of Storm Surge Barriers on Drag, Mixing, and Exchange Flow in a Partially Mixed
 912 Estuary. *Journal of Geophysical Research: Oceans*, 127(4), e2021JC018246.
 913 <https://agupubs.onlinelibrary.wiley.com/doi/abs/10.1029/2021JC018246>
- 914 Ralston, D. K., Cowles, G. W., Geyer, W. R., & Holleman, R. C. (2017). Turbulent and numerical mixing in a salt
 915 wedge estuary: Dependence on grid resolution, bottom roughness, and turbulence closure. *Journal of*
 916 *Geophysical Research: Oceans*, 122(1), 692-712.
 917 <https://agupubs.onlinelibrary.wiley.com/doi/abs/10.1002/2016JC011738>
- 918 Ralston, D. K., & Geyer, W. R. (2017). Sediment transport time scales and trapping efficiency in a tidal river.
 919 *Journal of Geophysical Research: Earth Surface*, 122(11), 2042-2063.
- 920 Ralston, D. K., & Geyer, W. R. (2019). Response to Channel Deepening of the Salinity Intrusion, Estuarine
 921 Circulation, and Stratification in an Urbanized Estuary. *Journal of Geophysical Research: Oceans*, 124(7),
 922 4784-4802. <https://agupubs.onlinelibrary.wiley.com/doi/abs/10.1029/2019JC015006>
- 923 Ralston, D. K., Geyer, W. R., & Lerczak, J. A. (2008). Subtidal Salinity and Velocity in the Hudson River Estuary:
 924 Observations and Modeling. *Journal of Physical Oceanography*, 38(4), 753-770.
 925 <http://dx.doi.org/10.1175%2F2007JPO3808.1>
- 926 Ralston, D. K., Warner, J. C., Geyer, W. R., & Wall, G. R. (2013). Sediment transport due to extreme events: The
 927 Hudson River estuary after tropical storms Irene and Lee. *Geophysical Research Letters*, 40(20), 5451-
 928 5455.
- 929 Rice, K. C., Hong, B., & Shen, J. (2012). Assessment of salinity intrusion in the James and Chickahominy Rivers as
 930 a result of simulated sea-level rise in Chesapeake Bay, East Coast, USA. *Journal of Environmental*
 931 *Management*, 111, 61-69. <https://www.sciencedirect.com/science/article/pii/S0301479712003519>
- 932 Rodenburg, L. A., & Ralston, D. K. (2017). Historical sources of polychlorinated biphenyls to the sediment of the
 933 New York/New Jersey Harbor. *Chemosphere*, 169, 450-459.
- 934 Schulte, J. A., Najjar, R. G., & Lee, S. (2017). Salinity and streamflow variability in the Mid-Atlantic region of the
 935 United States and its relationship with large-scale atmospheric circulation patterns. *Journal of Hydrology*,
 936 550, 65-79. <https://www.sciencedirect.com/science/article/pii/S002216941730210X>
- 937 Scully, M., Friedrichs, C., & Brubaker, J. (2005). Control of estuarine stratification and mixing by wind-induced
 938 straining of the estuarine density field. *Estuaries and Coasts*, 28(3), 321-326.
 939 <http://dx.doi.org/10.1007/BF02693915>
- 940 Swanson, R., O'Connell, C., & Wilson, R. (2013). *Storm Surge Barriers: Ecological and Special Concerns*. Paper
 941 presented at the Storm surge barriers to protect New York City: against the deluge, New York University,
 942 USA, 30-31 March 2009.

- 943 Tabak, N. M., Laba, M., & Spector, S. (2016). Simulating the Effects of Sea Level Rise on the Resilience and
944 Migration of Tidal Wetlands along the Hudson River. *Plos One*, 11(4), e0152437.
945 <https://doi.org/10.1371/journal.pone.0152437>
- 946 USACE. (2017). *Integrated City of Norfolk Coastal Storm Risk Management Feasibility Study*
947 *Report/Environmental Impact Statement* Norfolk
- 948 USACE. (2019). *New York-New Jersey Harbor and Tributaries Coastal Storm Risk Management Interim Report*,
949 *US Army Corps of Engineers New York District*. New York.
- 950 USACE. (2020a). "Assessing the effects of storm surge barriers on the hudson river estuary: Final Workshop",
951 presentation slides from United States Army Corps of Engineers, New York District at the workshop.
952 Retrieved from [https://philiporton.files.wordpress.com/2018/11/hat-presentation-for-orton-workshop-on-](https://philiporton.files.wordpress.com/2018/11/hat-presentation-for-orton-workshop-on-28-jan-20.pdf)
953 [28-jan-20.pdf](https://philiporton.files.wordpress.com/2018/11/hat-presentation-for-orton-workshop-on-28-jan-20.pdf)
- 954 USACE. (2020b). *Coastal Texas Protection and Restoration Feasibility Study*. Galveston.
- 955 USACE. (2020c). *Miami-Dade Back Bay Coastal Storm Risk Management Draft Integrated Feasibility Report*.
956 Norfolk
- 957 USACE. (2021a). *New Jersey Back Bays Coastal Storm Risk Management Study*. Philadelphia.
- 958 USACE. (2021b). *Reservoir Regulation Section Annual Report*. Retrieved from
959 https://reservoircontrol.usace.army.mil/nae_orcs/cwmsweb/cwms_web.other_html.BulletinPage
- 960 USACE. (2022). *NEW YORK-NEW JERSEY HARBOR AND TRIBUTARIES COASTAL STORM RISK*
961 *MANAGEMENT FEASIBILITY STUDY*. Retrieved from [https://www.nan.usace.army.mil/Missions/Civil-](https://www.nan.usace.army.mil/Missions/Civil-Works/Projects-in-New-York/New-York-New-Jersey-Harbor-Tributaries-Focus-Area-Feasibility-Study/)
962 [Works/Projects-in-New-York/New-York-New-Jersey-Harbor-Tributaries-Focus-Area-Feasibility-Study/](https://www.nan.usace.army.mil/Missions/Civil-Works/Projects-in-New-York/New-York-New-Jersey-Harbor-Tributaries-Focus-Area-Feasibility-Study/)
- 963 Wurtsbaugh, W. A., Paerl, H. W., & Dodds, W. K. (2019). Nutrients, eutrophication and harmful algal blooms along
964 the freshwater to marine continuum. *WIREs Water*, 6(5), e1373.
965 <https://wires.onlinelibrary.wiley.com/doi/abs/10.1002/wat2.1373>
- 966 Xie, X., & Li, M. (2018). Effects of Wind Straining on Estuarine Stratification: A Combined Observational and
967 Modeling Study. *Journal of Geophysical Research: Oceans*, 123.
- 968 Yuan, R., & Zhu, J. (2015). The Effects of Dredging on Tidal Range and Saltwater Intrusion in the Pearl River
969 Estuary. *Journal of Coastal Research*, 31(6), 1357-1362, 1356. [https://doi.org/10.2112/JCOASTRES-D-14-](https://doi.org/10.2112/JCOASTRES-D-14-00224.1)
970 [00224.1](https://doi.org/10.2112/JCOASTRES-D-14-00224.1)
- 971 Wahl, T., Jain, S., Bender, J. et al. Increasing risk of compound flooding from storm surge and rainfall for major US
972 cities. *Nature Clim Change* 5, 1093–1097 (2015). <https://doi.org/10.1038/nclimate2736>
- 973 United States Geological Survey National Water Information System (NWISWeb) online data,
974 <https://nwis.waterdata.usgs.gov/usa/nwis>, accessed December, 2021

975

976

977

978